Mathematisches Forschungsinstitut Oberwolfach

Report No. 37/2021

DOI: 10.4171/OWR/2021/37

Dynamics of Waves and Patterns (hybrid meeting)

Organized by
Margaret Beck, Boston
Martina Chirilus-Bruckner, Leiden
Christian Kühn, Garching
Jens Rademacher, Bremen

8 August – 14 August 2021

Abstract. The dynamics of waves and patterns play a significant role in the sciences, especially in fluid mechanics, material science, neuroscience and ecology. The mathematical treatment interconnects several areas, ranging from evolution equations and functional analysis to dynamical systems, geometry, topology, and stochastic as well as numerical analysis. This workshop has specifically focussed on dynamic stability on extended domains, bifurcations of waves and patterns, effects of stochastic driving, and spatio-temporal inhomogenities. During the workshop, multiple new directions, collaborations, and very interesting scientific conversations arose across the entire field.

Mathematics Subject Classification (2010): 35B36, 35B32, 35B35, 35C07.

Dedicated to the memory of Claudia Wulff

Introduction by the Organizers

The workshop *Dynamics of Waves and Patterns*, organised by Margaret Beck (Boston), Martina Chirilus-Bruckner (Leiden), Christian Kuehn (Garching) and Jens Rademacher (Bremen) was held as a hybrid meeting due to the covid19 pandemic, with 22 participants present in Oberwolfach, and more than 30 online participants from Europe, the Americas, Japan and Australia.

The workshop topic refers to phenomena that typically arise in the sciences, in particular fluid mechanics, material science, neuroscience and ecology. The mathematical treatment interconnects several areas, ranging from evolution equations and functional analysis to dynamical systems, geometry, topology, and stochastic as well as numerical analysis. The workshop has specifically focussed on the key areas

- Dynamic stability on extended domains
- Bifurcations of waves and patterns
- Effects of stochastic driving
- Spatio-temporal inhomogeneities

Stability and bifurcations are classical core themes in the field, but have undergone dramatic developments in recent years. The consideration of stochastic effects is a rapidly growing area, also beyond the proposed workshop theme, and closely related to the inclusion of spatio-temporal inhomogeneities, which appears as an emerging topic.

Due the special pandemic circumstances, we make some comments on organisation and technical realisation. It is worth noting that for all participants present at MFO it was the first workshop in presence since one or even two years.

The workshop had to be organized in hybrid format so that we have implemented special measures in order to keep a sense of community. This was particularly important due to the split of the audience into roughly the same number of virtual as well as live participants. We have been happy to see that virtual participation was extremely steady and consistent across the entire week with almost all participants being present for all the talks. In addition to the excellent MFO hybrid setup with cameras and screens, we have conducted discussions on an online mural board, which were very successful in collecting current and new directions of the field. Furthermore, we provided the option for online social interaction sessions after the main set of talks (gather.town), which also were well attended. In summary, we were very positively surprised, how well the hybrid format worked, although clearly most online participants, who could not attend due to travel restrictions, did miss the MFO atmosphere considerably.

During the workshop, multiple new directions, collaborations, and very interesting scientific conversations arose across the entire field of pattern formation in spatial systems. We believe that we have succeeded as proposed in establishing new components into the field such as pattern formation in stochastic partial differential equations as well as spatio-temporally heterogeneous systems. We consider these directions as extremely important from a mathematical viewpoint as they can interlink PDE theory much better with stochastic analysis, with non-autonomous techniques from low-dimensional dynamics and control, as well as with interacting particle systems creating spatial heterogeneity. Of course, many pattern formation problems arising in various application areas such as the life science or geophysics, also have to deal with stochastic perturbations and/or spatio-temporal heterogeneity. Building upon the solid core of the field and the newly established directions, the workshop has helped tremendously to identify future challenges.

More specifically, we summarize the synthesis of the open discussion sessions, which were wonderfully chaired by Jon Dawes – thanks Jon! Our goal was to identify aspects of the field that appear to be currently (still) highly relevant, active or emerging, that may be further developed to lead to a guideline for students and early career scientists. Clearly, this was a deeply subjective selection and far from fully worked out. We have organised the contributions into five themes as follows, wherein part of the keywords are a mix of aspects that reappeared in the talks of the workshop and thus may simply reflect the choice of speakers, but that we also found to be used in new ways:

- *Methods.* Infinite dimensional invariant manifolds, (geometric) singular perturbation theory, bifurcations, travelling waves and spatial dynamics, collective coordinates, functional analytic tools, rigorous as well as structure preserving numerics.
- *Dynamics.* Transients, metastability, transitions, localised phenomena, freak waves.
- *Heterogeneity* Time-dependence and non-autonomous systems, spatial heterogeneity, stochastic dynamics, robustness, control.
- *Structure.* Agent based modelling, cellular automata, particles, networks and differential equations arising from graph limit, geometric/manifold domain effects, cross diffusion.
- *Applications/Transfer.* Stochastics, data assimilation (slow-fast), machine learning, climate (examples from different modelling complexity scales), life sciences esp. pharmacology, communication, critical transitions, epidemiology and socio-economic models (and connections to optimal control).

Acknowledgement: The workshop organizers thank the MFO for the wonderful hospitality in this pandemic time.

Workshop (hybrid meeting): Dynamics of Waves and Patterns

Table of Contents

Abstracts

Approximately invariant manifolds

Dirk Blömker
(joint work with Alexander Schindler)

We follow ideas partially presented in [8] and consider the dynamics along a manifold $\mathcal{M}$ of a solution u of a stochastic partial differential equation of the type

$$\text{(SPDE)} \qquad \partial_t u = \mathcal{L}_\varepsilon(u) + \partial_t W_\epsilon,$$

where W_ϵ is a Wiener-process corresponding to small Gaussian noise and $\mathcal{L}_\varepsilon$ a deterministic drift. Here both might depend on a small parameter $\epsilon > 0$. We assume that u is a local solution of (SPDE), which is a stochastic process with continuous paths in a Hilbert-space $\mathcal{H}$ that might only exist up to a blow-up time. Let

$$\mathcal{M} := \{u^h \ : \ h \in \mathcal{P}\}$$

be a smooth non-degenerate N-dimensional manifold on an open parameter space $\mathcal{P} \subset \mathbb{R}^N$. Typical examples are travelling waves [6, 7] where $\mathcal{M}$ is one dimensional and given by translations of the front. Other examples are the metastable kink motion in one-dimensional Allen-Cahn/Cahn-Hilliard equations[2, 5] or the motion of a single bubble [1, 4]. Here the manifold is parametrised by the position of the interfaces or the center of the bubble. But there are many more examples that would fit into this framework, like spiral waves or the motion along a center manifold close to bifurcation [3].

1. Formal Derivation of the SDE on $\mathcal{M}$. Assuming that we have a well defined coordinate system where $u = u^h + v$ with $v \perp \mathcal{M}$ (i.e., $\langle v, \partial_j u^h \rangle = 0$ for all $j = 1, \dots, N$) and assuming that h is a diffusion in $\mathcal{P}$ we can derive a stochastic differential equation of the following type:

$$\text{(SDE)} \qquad A(h,u)dh = F(h,u)dt + G(h,u)dW_\epsilon$$

where the matrix $A(h,u) \in \mathbb{R}^{N\times N}$ is given by $A(h,u)_{i,j} = \langle \partial_j u^h, \partial_i u^h \rangle - \langle \partial_{ij} u^h, v \rangle$, where we define $v = u - u^h$.

2. Results. The matrix A, as well as the drift F and the diffusion G, are locally Lipschitz in h and continuous in time, thus we can prove the following:

Theorem 1: *Given the solution u and an $h(0) \in \mathcal{P}$ there is a unique local solution of (SDE) up to a stopping time where either*

- *$A(h,v)^{-1}$ does not exist*
- *h reaches the boundary of $\mathcal{P}$ or ∞ (i.e., the pattern breaks down)*
- *the solution u fails to exist*

Reverting the formal calculation that leads to (SDE) one can prove

Theorem 2: *Let u be the solution of (SPDE) as above and h the solution of (SDE) of the previous theorem such that $h(0) \in \mathcal{P}$ and $v(0) := u(0) - u^{h(0)} \perp \mathcal{M}$ then $v(t) := u(t) - u^{h(t)} \perp \mathcal{M}$ for all times where h exists.*

Let us remark that initially one can often take a (not necessarily unique) point of smallest distance to the manifold in order to derive $h(0)$ and $v(0)$.

Let us point out that the invertibility of A is a purely geometric constraint independent of the parametrisation of the manifold and the dynamics of the manifold. Due to the fact that the manifold is non-degenerate one easily observes that the matrix A is invertible if v is sufficiently small.

3. Stability. If v is sufficiently small (i.e., u close to $\mathcal{M}$) then not only we have a well defined reduced process h on $\mathcal{P}$ but we can also derive a simplified model from (SDE) by removing the u.

Thus let us look closer on an equation of v in the Stratonovic sense

$$\begin{aligned} dv &= du - d(u^h) \\ &= \mathcal{L}_\epsilon(u^h - v)dt + \circ dW_\epsilon - \sum_j \partial_j u^h \circ dh_j \\ &= \Big[\mathcal{L}_\epsilon(u^h) + D\mathcal{L}_\epsilon(u^h)v + N(h,v)\Big]dt + \circ dW_\epsilon - \sum_j \partial_j u^h \circ dh_j \end{aligned}$$

while the nonlinearity is higher order in v the crucial terms are first the operator $\mathcal{L}(u^h)$, which should be small normal to the manifold, and secondly the linearised operator, which should be stable normal to the manifold. It would be sufficient if $\langle \mathcal{L}_\epsilon(u^h), v\rangle$ is smalll and we have good control of the quadratic form $\langle D\mathcal{L}_\epsilon(u^h)v, v\rangle$ for $v \perp \mathcal{M}$ and $h \in \mathcal{P}$.

One usually expects solutions to be on the order of noise strength divided by the square root of the linear attraction rate for very long times until either h leaves $\mathcal{P}$ or large deviation effects like nucleation set in.

References

[1] D. C. Antonopoulou, P. W. Bates, D. Blömker, G. D. Karali, *Motion of a droplet for the mass-conserving stochastic Allen-Cahn equation*, SIMA **48**(1), (2016), 670–708

[2] D. C. Antonopoulou, D. Blömker, G. D. Karali, *Front Motion in the One-Dimensional Stochastic Cahn-Hilliard Equation*, SIMA **44**, (2012), 3242–3280

[3] D. Blömker, M. Hairer, *Amplitude Equations for SPDEs: Approximate Centre Manifolds and Invariant Measures* in: Probability and Partial Differential Equations in Modern Applied Mathematics, ed. by Edward C. Waymire and Jinqiao Duan, (IMA Vol. in Math. and its Appl. ; 140), (2005), 41–59

[4] D. Blömker, A. Schindler, *Stochastic Cahn–Hilliard equation in higher space dimensions: the motion of bubbles*, Z. Angew. Math. Phys, **71**, (2020), 49

[5] D. Blömker, A. Schindler, *Kink motion for the one-dimensional stochastic Allen-Cahn equation*, ArXiv, (2021)

[6] M. Cartwright, G. A. Gottwald, *A collective coordinate framework to study the dynamics of travelling waves in stochastic partial differential equations*, Phys. D, **397**, (2019), 54–64

[7] C. H. S. Hamster, H. J. Hupkes, *Stability of traveling waves on exponentially long timescales in stochastic reaction-diffusion equations*, SIAM J. Appl. Dyn. Syst., **19**(4), (2020), 2469–2499

[8] A. Schindler, *Interface motion for the stochastic Allen–Cahn and Cahn–Hilliard equation*, PhD thesis, Universität Augsburg, (2021)

Multistability and time-periodic spatial pattern in the cross-diffusion SKT model

Cinzia Soresina

The Shigesada–Kawasaki–Teramoto model (SKT) was proposed to account for stable inhomogeneous steady states exhibiting spatial segregation, which describes a situation of coexistence of two competing species. Even though the reaction part does not present the activator-inhibitor structure, the cross-diffusion terms are the key ingredient for the appearance of spatial patterns. We provide a deeper understanding of the conditions required on both the cross-diffusion and the reaction coefficients for non-homogeneous steady states to exist [1], by combining a detailed linearised with advanced numerical bifurcation methods via the continuation software `pde2path`. We study the role of the additional cross-diffusion term in pattern formation, showing that the cross-diffusion terms have an opposite effect. However, the bifurcation structure undergoes major deformations when the interspecific competition pressure is increased, revealing changes, non predicted by the linearized analysis, in the type of pitchfork bifurcations on the homogeneous branch, leading to multistability regions, as well as in the presence of Hopf bifurcation points. Through weakly nonlinear analysis we can predict the type of pitchfork bifurcation and the change from super- to sub-critical, leading to the appearance of a multi-stability region. In the weak-competition case, the interspecific competition pressure also influences the possible appearance of stable time-period spatial patterns. In fact, by performing a three-parameter analysis, we detect the presence of a codimension-3 bifurcation point, at which the bifurcation structure drastically changes. This point is located at the intersection of the neutral stability curves (curves of pitchfork bifurcation points) related to the 1- and 2-mode, at which also the Landau coefficient changes sign. When the additional cross-diffusion coefficient is small, the system presents stable time-periodic spatial patterns arising through a Hopf bifurcation point. When the additional cross-diffusion coefficient is increased, we detect Hopf bifurcations in a larger region of the parameter space, but the time-periodic spatial patterns seem to be unstable. This can be also studied through center manifold reduction, considering the reduced and truncated system which describes the PDEs system close to the degenerate point.

Thanks to its interplay between linearized analysis, weakly nonlinear analysis and numerical continuation, this work constitutes a step forward in the analytical understanding of the bifurcation structure of the SKT system, it points out new interesting aspects and opens several different questions that can be addressed in future works.

A stronger characterisation of the doubly degenerate point at the critical value is needed at this point. This would also allow progress in the understanding of the time-periodic spatial patterns which potentially originate in the vicinity of the doubly degenerate point. While the analytical approach may be feasible, the continuation software `pde2path` is not immediately suited for the detection of codimension-2 bifurcation points, so this will be a matter of future investigations.

On the other side, it would also be interesting to investigate how far from the doubly degenerate point and why the Hopf bifurcation point and of the time-periodic spatial patterns disappear. From the ecological viewpoint, the influence of the domain size on the type of stable steady and time-periodic patterns is crucial. It is not clear if the domain size has an influence only on the solution profiles (due to different unstable modes), or it can even induce major deformations of the bifurcation structure. It has also been shown the presence of stable non-homogeneous solutions outside the parameter region in which the homogeneous state exists (positive) [4], which constitutes an extremely interesting effect of cross-diffusion not yet investigated. Another important direction is the study of the strong competition case. In [1] it has been shown an interesting effect of the additional cross-diffusion term on the bifurcation structure and the presence of Hopf bifurcation points. Better characterization and a deeper investigation would improve the understanding of this different regime. Note that the derivation of the Stuart–Landau equation and the weakly nonlinear analysis holds and it can predict the type of pitchfork bifurcation on the homogeneous branch also in the strong-competition regimes. Moreover, an extremely interesting and actual research direction is the extension of cross-diffusion induced instability on networks, that we are currently investigating [5]. Finally, the same study could be carried out for other quasilinear problems involving cross-diffusion terms. For instance, it is possible to derive by time-scale arguments a different type of cross-diffusion in predator–prey systems,[2, 3]. The linearized analysis already suggests that they do not increase the parameter region in which patterns appear, but the global influence of these terms cannot be captured only by the linearized analysis. Taken together, these results will better clarify the role of cross-diffusion terms as the key ingredients in pattern formation.

References

[1] M. Breden, C. Kuehn, C. Soresina, *On the influence of cross-diffusion in pattern formation*, Journal of Computational Dynamics **8.2** (2021), 213.

[2] F. Conforto, L. Desvillettes, C. Soresina, *About reaction–diffusion systems involving the Holling-type II and the Beddington–DeAngelis functional responses for predator–prey models*, Nonlinear Differential Equations and Applications **25.3** (2018), 1–39.

[3] L. Desvillettes, C. Soresina, *Non-triangular cross-diffusion systems with predator-prey reaction terms*, Ricerche di Matematica **68.1** (2019), 295–314.

[4] C. Kuehn, C. Soresina, *Numerical continuation for a fast-reaction system and its cross-diffusion limit*, SN Partial Differential Equations and Applications **1.2** (2020), 1–26.

[5] C. Kuehn, C. Soresina, *Cross-diffusion induced instability on networks*, in preparation.

[6] C. Soresina, *Hopf bifurcation in the full SKT model and where to find them*, under review, 2021.

Global dynamics of a nonconservative nonlinear Schrödinger equation

Jonathan Jaquette
(joint work with Jean-Philippe Lessard, Akitoshi Takayasu)

In this talk we discuss the nonlinear Schrödinger equation

$$iu_t = \triangle u + u^2, \qquad x \in \mathbb{T} \equiv \mathbb{R}/\tfrac{2\pi}{\omega}\mathbb{Z} \tag{1}$$

This NLS does not have gauge invariance, $(e^{i\theta}u)^2 \neq e^{i\theta}u^2$ for generic $\theta \in \mathbb{R}$, and it does not admit a natural Hamiltonian structure.

A precursor to (1) can be seen in the work of Masuda [1, 2] who studied the blowup of solutions to the real PDE $u_t = \triangle u + u^2$. By extending solutions with close-to-constant initial data in the complex plane of time, Masuda was able to extend past the blowup point and demonstrate a branching singularity. This approach was continued for non-close-to-constant initial data in the numerical work [3, 4].

Equation (1) arises from $u_t = \triangle u + u^2$ by solving the equation in a purely imaginary direction of time. From their numerics, Cho et al. conjectured that real initial data to (1) is globally well posed [3]. For close-to-constant real initial data this is shown to be the case [5]. When restricting (1) to constant initial data one obtains the ODE $i\dot{z} = z^2$, whereby 0 is foliated by homolcinic solutions, with the exception of some finite time blowup solutions. In fact, these homoclinic solutions can be robustly extended to an open set.

Theorem 1 ([5]). *There exists an open set of complex initial data with summable Fourier coefficients whose solutions are homoclinic orbits, limiting to* 0 *in both forward and backward time.*

Note that if there exists some continuous conserved quantity H, it would necessarily be constant on this open set and equal to $H(0)$. Moreover, if H was analytic then it would have to be globally constant; ie (1) is nonconservative.

Corollary 2 ([5]). *The only analytic functionals conserved under* (1) *are constant.*

Indeed, a significant portion of the dynamics can be seen to mimic the spatially homogeneous dynamics. However this is not the only dynamics possible.

Theorem 3 ([5]). *There exist at least two non-trivial equilibria to* (1)*, each of whose linearization has at least one unstable eigenvalue.*

Moreover, due to the rescaling of solutions $u(t, x) \mapsto n^2 u(n^2 t, nx)$, these two equilibria generate two infinite families of unstable equilibria. It appears that as n increases so does the number of unstable eigenvalues in the equilibrium's linearization increases. However formalizing this relation, and also classifying all of the equilibria to (1), remains open.

By way of computer assisted proofs, we are able to demonstrate heteroclinic orbits to and from these nontrivial equilibria.

Theorem 4 ([5]). *For each equilibrium $\tilde{u}$ in Theorem 3, there exists a heteroclinic orbit u_a traveling from $\tilde{u}$ to* 0*, and a heteroclinic orbit u_b traveling from* 0 *to $\tilde{u}$.*

The heteroclinic u_a is proved using validated numerics. We first develop a high order approximation of the unstable manifold using the parameterization method in the case of PDEs (cf [6]). Next we use the validated integrator adapted from [4] to propagate these solutions forward in time. This is continued until the trajectory enters an explicit trapping region (an open set) of solutions which converge to 0. The heteroclinic u_b follows from the time reversal symmetry of conjugate solutions.

The unstable manifold of the two nontrivial equilibria in Theorem 3 has complex dimension of at least 1, and most of those trajectories appear to be heteroclinic orbits limiting to 0. However numerics suggest there exists an isolated trajectory in the unstable manifold which grows without bound [7]. In similar equations to (1) with added dissipation, we prove the existence of unbounded solutions using a forcing argument from [8]. However this does not distinguish between blowup and growup, and the forcing argument does not apply to the NLS case of (1).

In addition to the dynamics already demonstrated, one might ask if there exists any recurrent dynamics? To answer this, we look at the space of initial data with non-negative Fourier coefficients, which in fact forms an integrable subsystem.

Theorem 5 ([9])**.** *The initial data* $u_0(x) = \sum_{n \in \mathbb{N}} \phi_n e^{i\omega n x}$*, with* $\sum_{n\in\mathbb{N}} |\phi_n| < \infty$ *has a solution to* (1) *given by*

$$u(t,x) = \sum_{n \in \mathbb{N}} a_n(t) e^{i\omega n x} \tag{2}$$

where each function $a_n(t)$ *may be solved for explicitly by quadrature.*

While equation (1) does not admit a standard Hamiltonian structure, this integrable subspace suggests there may exist some singular conserved quantities or a singular symplectic structure, cf [10, 11]. One may also compare this subsystem to the cubic Szegő equation, another PDE defined on non-negative Fourier coefficients and shown to be integrable [12].

For examples of solutions in this subspace, consider monochromatic initial data.

Example 6 ([9])**.** *Fix* $A \in \mathbb{C}$*,* $\omega > 0$ *and initial data* $u_0(x) = Ae^{i\omega x}$*. The first few functions* $a_n : \mathbb{R} \to \mathbb{C}$ *in* (2) *are given as follows*

$$\begin{aligned}
a_1(t) &= Ae^{i\omega^2 t} \\
a_2(t) &= \frac{A^2}{\omega^2}\left(\frac{1}{2}e^{2i\omega^2 t} - \frac{1}{2}e^{4i\omega^2 t}\right) \\
a_3(t) &= \frac{A^3}{\omega^4}\left(\frac{1}{6}e^{3i\omega^2 t} - \frac{1}{4}e^{5i\omega^2 t} + \frac{1}{12}e^{9i\omega^2 t}\right) \\
a_4(t) &= \frac{A^4}{\omega^6}\left(\frac{7e^{4i\omega^2 t}}{144} - \frac{e^{6i\omega^2 t}}{10} + \frac{e^{8i\omega^2 t}}{32} + \frac{e^{10i\omega^2 t}}{36} - \frac{11e^{16i\omega^2 t}}{1440}\right)
\end{aligned}$$

Note that each function $a_n(t)$ is given by $A^n/\omega^{2(n-1)}$, multiplied by a $2\pi/\omega^2$ periodic function. Given this geometric scaling, one may expect that if the ratio is very small then the solution will converge to a periodic orbit, and if the ratio is very large then the solution will blowup. This is indeed the case.

Theorem 7 ([9]). *Consider the solution from Example 6.*

- *If $A/\omega^2 < 3$ then the solution is periodic with period $2\pi/\omega^2$.*
- *If $A/\omega^2 \geq 6$ then the solution blows up in finite time in the L^2 norm.*

The lower value of 3 was obtained by computer assisted proof, and the upper value of 6 was obtained with pen-and-paper. Using non-validated numerics we estimate that the critical dividing line between periodic orbits and blowup is approximately $A/\omega^2 \approx 3.37$. We also note that the periodic orbits here all have a fixed frequency which does not depend on their amplitude. This is in fact true for more general initial data supported on positive Fourier coefficients.

Theorem 8 ([9]). *Fix initial data $u_0(x) = \sum_{n=1}^{\infty} \phi_n e^{i\omega n x}$. If $\sum_{n=1}^{\infty} |\phi_n| < \frac{\omega^2}{4}$ then the solution is periodic with period $2\pi/\omega^2$.*

In summary, the evolutionary equation (1) supports rich dynamics with varied behavior. Some trajectories are periodic and others limit to equilibria. Some solutions have global existence and others blowup in finite time.

References

[1] K. Masuda, *Blow-up of solutions of some nonlinear diffusion equations.* In North-Holland Mathematics Studies, **81**, pp. 119-131. North-Holland, 1983.

[2] K. Masuda, *Analytic solutions of some nonlinear diffusion equations.* Mathematische Zeitschrift **187**, no. 1 (1984): 61-73.

[3] C.H. Cho, H. Okamoto, and M. Shōji, *A blow-up problem for a nonlinear heat equation in the complex plane of time.* Japan Journal of Industrial and Applied Mathematics **33**, no. 1 (2016), 145-166.

[4] A. Takayasu, J.P. Lessard, J. Jaquette, and H. Okamoto, *Rigorous numerics for nonlinear heat equations in the complex plane of time.* arXiv preprint arXiv:1910.12472 (2019).

[5] J. Jaquette, J.P. Lessard, and A. Takayasu, *Global dynamics in nonconservative nonlinear Schrödinger equations.* arXiv preprint arXiv:2012.09734 (2020).

[6] C. Reinhardt, and J.D. Mireles James, *Fourier-Taylor parameterization of unstable manifolds for parabolic partial differential equations: formalism, implementation and rigorous validation.* Indagationes Mathematicae **30**, no. 1 (2019): 39-80.

[7] J. Jaquette, J.P. Lessard, and A. Takayasu, *Singularities and heteroclinic connections in complex-valued evolutionary equations with a quadratic nonlinearity.* arXiv preprint arXiv:2109.00159 (2021).

[8] H. Stuke, *Complex time blow-up of the nonlinear heat equation.* arXiv preprint arXiv:1812.10707 (2018).

[9] J. Jaquette, *Quasiperiodicity and blowup in integrable subsystems of nonconservative nonlinear Schrödinger equations.* arXiv preprint arXiv:2108.00307 (2021).

[10] V. Guillemin, E. Miranda, and A.R. Pires. *Symplectic and Poisson geometry on b-manifolds.* Advances in mathematics **264** (2014), 864–896.

[11] R. Braddell, A. Delshams, E. Miranda, C. Oms, and A. Planas. *An invitation to singular symplectic geometry.* International Journal of Geometric Methods in Modern Physics **16**, no. supp01 (2019), 1940008.

[12] P. Gérard and S. Grellier, *Invariant tori for the cubic Szegö equation.* Inventiones mathematicae **187** no. 3 (2012), 707–754.

The influence of autotoxicity on the dynamics of vegetation spots

Annalisa Iuorio
(joint work with Frits Veerman)

Plant autotoxicity has proved to play an essential role in the behaviour of local vegetation [1, 2]. We analyse a reaction-diffusion-ODE model describing the interactions between vegetation, water, and autotoxicity originally proposed in [3]. The presence of autotoxicity is seen to induce movement and deformation of spot patterns in some parameter regimes, a phenomenon which does not occur in classical biomass-water models (see Figure 1).

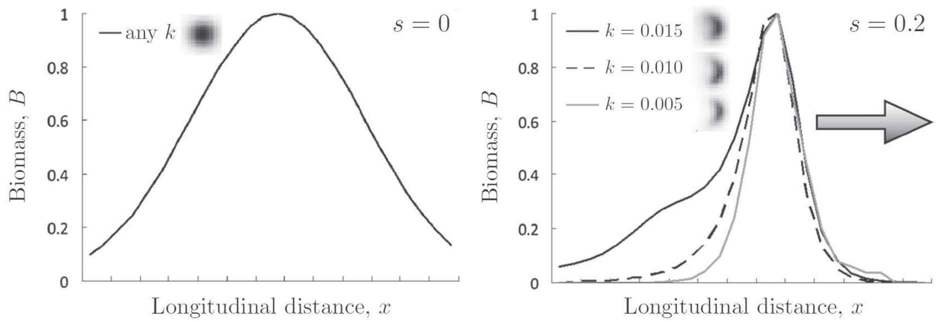

Figure 1. Cross section of a single biomass spot in relation to two main parameters, i.e. plant sensitivity to toxicity (s) and toxicity decay rate (k). When plants dynamics are assumed to be decoupled from toxicity (i.e. in the case $s = 0$, left panel), a stable isolated vegetation spot has a symmetric distribution of biomass with a peak in its center. On the other hand, the negative feedback induced by toxicity (i.e. $s \neq 0$, in particular $s = 0.2$ in the right panel) modifies the shape of the biomass curve within a continuously moving vegetation spot. The intensity of such effect is displayed for three levels of k, and the arrow indicates the direction of the moving biomass front. The top-left corner of each panel shows the appearence of the corresponding pattern in 2D.

We aim to analytically quantify this novel feature, by studying travelling wave solutions in one spatial dimension. In [4], we use geometric singular perturbation theory to prove the existence of symmetric, stationary and non-symmetric, travelling pulse solutions, by constructing appropriate homoclinic orbits in the associated 5-dimensional dynamical system. In the singularly perturbed context, we perform an extensive scaling analysis of the dynamical system, identifying multiple asymptotic scaling regimes where (travelling) pulses may or may not be constructed. We discuss the agreement and discrepancy between the analytical results and numerical simulations. Our findings indicate how the inclusion of an additional ODE may significantly influence the properties of classical biomass-water models of Klausmeier/Gray–Scott type.

Recently, a successful collaboration with Arjen Doelman (U. Leiden) and Paul Carter (U. Minnesota) has lead to the resolution of the above mentioned discrepancy between numerical and analytical travelling pulses. In particular, the numerically observed travelling pulse has proved to be, in a certain sense, a perturbation of the "regular" planar homoclinic in classical biomass-water models. Currently, we are working on the stability of such structures using an approach based on the Evans function.

Our next goals are:

- Perform a thourough bifurcation analysis using the continuation tool `AUTO`;
- Consider logistic effects in the dynamics of vegetation and explore the corresponding modifications in the travelling pulse structure;
- Investigate existence and stability of double-scale patterns, where a larger, stable pattern forms within which another dynamic patterned structure persists. Such objects are of particular interest as they appear in many different biological/ecological applications (e.g. mussel beds).

References

[1] F. Cartenì, A. Marasco, G. Bonanomi, S. Mazzoleni, M. Rietkerk, and F. Giannino, *Negative plant soil feedback explaining ring formation in clonal plants*, Journal of Theoretical Biology **313** (2012), 153–161.

[2] S. Mazzoleni, G. Bonanomi, F. Giannino, G. Incerti, S.C. Dekker, and M. Rietkerk, *Modelling the effects of litter decomposition on tree diversity patterns*, Ecological Modelling **221(23)** (2010), 2784–2792.

[3] A. Marasco, A. Iuorio, F. Cartenì, G. Bonanomi, D.M. Tartakovsky, S. Mazzoleni, and F. Giannino, *Vegetation pattern formation due to interactions between water availability and toxicity in plant-soil feedback*, Bulletin of Mathematical Biology **76** (2014), 2866–2883.

[4] A. Iuorio, F. Veerman, *The influence of autotoxicity on the dynamics of vegetation spots*, bioRxiv 2020.07.29.226522 (to appear on Physica D: Nonlinear Phenomena) (2020).

Localized patterns on graphs: The influence of dimension and topology on pattern formation

Jason J. Bramburger

(joint work with Björn Sandstede)

The competition between bistable states in nonlinear systems can lead to localized structures with a patterned or activated state inside of a compact spatial region and a second homogeneous state outside of this compact region. Localized structures of this kind can be found in many applications, including as crime hotspots, vegetation patterns, and soft matter quasicrystals. They have further been observed in chemical reactions, supported elastic struts, semiconductors, and ferrofluids [5, 6]. What has become clear is that the spatial setting in which these pattern-forming systems are posed upon plays an integral role in determining what kinds of localized patterns can be observed and how these patterns are arranged in parameter space. To better understand this interplay between space and structure we have elected to investigate spatially-discrete reaction-diffusion equations of the form

$$\dot{u}_n = d(\Delta u)_n + f(u_n, \mu), \quad n \in \Lambda \tag{1}$$

where Δ is a discrete graph Laplacian which encodes the topological organization of the discrete space, indexed by the countable set Λ. The question then becomes: for a given pair (Λ, Δ), what types of steady-state patterns does (1) exhibit and what happens to these patterns as we vary the parameter $\mu \in \mathbb{R}$.

Our investigation of (1) begins by considering the one-dimensional integer lattice $\Lambda = \mathbb{Z}$ with nearest-neighbour interactions: $(\Delta u)_n = u_{n+1} + u_{n-1} - 2u_n$ for all n. In this case the existence of steady localized solutions can equivalently be posed as the existence of homoclinic orbits in a related two-dimensional mapping. Thus, we are able to extend the methods of [1] to construct these homoclinic orbits using Lin's method in the given mapping. Our results have shown that upon varying μ, these localized structures exhibit a bifurcation scenario known as *snaking* whereby unbounded existence curves bounce back and forth between two fixed values of μ [3]. Moving along this existence curve one sees the region of localization increasing in a regular manner as one rounds the fold bifurcations that mark the left and right extremities of the curve. A follow-up investigation has shown that localized states with multiple disjoint regions of localization do not exhibit snaking, but lie on closed existence curves called *isolas* [2].

For higher-dimensional lattice structures and/or more complex interactions, the spatial dynamics perspective of viewing localized patterns of (1) as homoclinic orbits of a mapping is lost. In the case of $\Lambda = \mathbb{Z}^2$ and nearest-neighbour connections in Δ, numerical investigations have shown that the existence curves are much more complicated than the 1D lattice setting [8] and bear a striking resemblance to localized planar hexagon patches found in the Swift–Hohenberg equation [7]. To understand this analytically we can take advantage of the fact that when $d = 0$ in (1) the system completely decouples, allowing one to provide an analytical explanation of the existence curves with $\Lambda = \mathbb{Z}^2$ for $0 < d \ll 1$ using Lyapunov–Schmidt reduction. These investigations have demonstrated that the dimension of the lattice and the connection topology in Δ plays a crucial role in the expected bifurcation diagrams of localized solutions. Then, to better understand the influence of connection topology, we turn to (1) on a finite ring [9]. We find that on a N element ring with nearest-neighbour coupling leads to existence curves with $2N$ folds along the branch, while all-to-all coupling always results in a closed curve emerging from a homogeneous state with exactly five folds, regardless of ring size.

These are initial steps towards a greater understanding of the integral role that spatial organization can have on pattern formation, and the accessibility of (1) with $d \approx 0$ provides the optimal setting to gain such insight. The aforementioned investigations have all used regular graph topologies to achieve their results, and therefore moving forward one wishes to investigate localized pattern formation on arbitrary or even random graphs. It is likely that completely general statements are not accessible, but there are promising avenues to understand patterns on large, random graphs using graphons. Results in this directions will be reported by the author soon.

References

[1] M. Beck, J. Knobloch, D. Lloyd, B. Sandstede, and T. Wagenknecht, *Snakes, ladders, and isolas of localized patterns*, SIAM J. Math. Anal. **41** (2009) 936-972.

[2] J.J. Bramburger, *Isolas of multi-pulse solutions to lattice dynamical systems*, Proc. R. Soc. Edin. A-Ma. **151** (2021) 916-952.

[3] J.J. Bramburger and B. Sandstede, *Spatially localized structures in lattice dynamical systems* J. Nonlinear Sci. **30**, (2020) 603-644.

[4] J.J. Bramburger and B. Sandstede, *Localized patterns in planar bistable weakly coupled lattice systems* Nonlinearity **33**, (2020) 3500-3525.

[5] J.H.P. Dawes, *The emergence of a coherent structure for coherent structures: Localized states in nonlinear systems*, Philos. Trans. R. Soc. Lond. Ser. A **368** (2010), 3519-3534.

[6] E. Knobloch. *Spatial localization in dissipative systems*, Ann. Rev. Condens. Matter Phys. **6** (2015) 325-359.

[7] D.J.B. Lloyd, B. Sandstede, D. Avitabile, A.R. Champneys, *Localized hexagon patches of the planar Swift–Hohenberg equation* SIAM J. Appl. Dyn. Syst. **7** (2008) 1049-110.

[8] C. Taylor and J.H. Dawes, *Snaking and isolas of localised states in bistable discrete lattices*, Phys. Lett. A **375** (2010) 14-22.

[9] M. Tian, J.J. Bramburger, and B. Sandstede, *Snaking bifurcations of localized patterns on ring lattices* IMA J. Appl. Math. at press

Traveling pulses with oscillatory tails, figure-eight-like stack of isolas, and dynamics in heterogeneous media

Yasumasa Nishiura

(joint work with Takeshi Watanabe)

1. Outline

The interplay between 1D traveling pulses with oscillatory tails (TPO) and heterogeneities of bump type is studied for a generalized three-component FitzHugh-Nagumo (GFN) equation. We first present that stationary pulses with oscillatory tails (SPO) form a "snaky" structure in homogeneous space, then TPO branches take a form of "figure-eight-like stack of isolas" located adjacent to the snaky structure of SPO. Here we adopt input resources such as voltage-difference as a bifurcation parameter. A drift bifurcation from SPO to TPO can be found by introducing another parameter at which these two solution sheets merge. As for the heterogeneous problem, in contrast to monotone tail case, there appears a nonlocal interaction between the TPO and the heterogeneity that creates infinitely many saddle solutions and finitely many stable stationary solutions distributed on the whole line. The response of TPO shows a variety of dynamics including pinning and depinning processes in addition to penetration (PEN) and rebound (REB). Stable/unstable manifolds of these saddles interact with TPO in a complex way, which causes a subtle dependence on the initial condition and a difficulty to predict the behavior after collision even in one-dimensional space. Nevertheless, for 1D case, a systematic global exploration of solution branches induced by heterogeneities (heterogeneous-induced-ordered patterns, HIOP for brevity) unveils that HIOP contains all the asymptotic states after collision so that we can predict the fate of the solution without solving the PDEs. The reduction method to finite-dimensional ODEs allow us to clarify the detailed mechanism of the transitions from PEN to pinning and pinning to REB from dynamical system view point. It turns out that the basin boundary between two different outputs against the heterogeneities forms an infinitely many successive reconnection of heteroclinic orbits among those saddles as the strength of heterogeneity is increased, which causes aforementioned subtle dependence of initial condition. For details, see [1].

2. Why three-component system?

We are interested in the interactive dynamics of localized traveling patterns with other objects such as collision against similar patterns or heterogeneities (or defects) in the media. Three-component system is necessary to ensure the coexistence of stable localized patterns in 2D or 3D. Suppose three components consist of one activator and two inhibitors, then the first inhibitor controls the width of front-rear direction and the second one does that of right and left direction. Two-component system does not support the coexistence of stable traveling patterns in higher dimensional space, simply because it cannot control the width of right and left direction and the pattern either elongates or shrinks depending on parameters. One representative three-component model is GFN system consisting of one activator and two inhibitors, in which the second inhibitor is responsible for controlling the shape orthogonal to propagating direction. As a first step, we investigate one-dimensional case and focus on the collision dynamics against the heterogeneity of bump type.

3. Why oscillatory tail?

When a localized pattern has an oscillatory tail, then it has a wave-like property, namely it can interact remotely with other localized patterns and heterogeneities (or defects) both in attractive and repulsive manners, which makes a sharp contrast with monotone tail case. The remote interaction causes a variety of coherent patterns and dynamics such as bound states (or molecules), crystal structure, various outputs via collision with heterogeneity. The main body of the localized traveling pattern can be regarded as a particle and we can identify its location and velocity by measuring the motion of it, which has a great advantage in the sense that it allows us to reduce the complex PDE dynamics into a finite-dimensional ODE system with an inhomogeneous term of oscillatory nature.

4. Figure-eight-like stack of isolas

The set of traveling pulse solutions forms a figure-eight-like stack of isolas with respect to an appropriate parameter so that there is an admissible region from one saddle to another saddle in which stable traveling pulse is observed. Such a structure merges into a solution set of standing pulse that forms a well-known snakes-and-ladders structure when another parameter tends to a drift bifurcation point. Loosely speaking, figure-eight-like structure is a kind of imperfection of snakes-and-ladders one.

5. Oscillatory tail interacts with heterogeneity

Once we introduce a heterogeneity into media, the interaction between traveling pulses and heterogeneity produces a variety of interesting dynamics including rebound, pinning, and even chaotic behavior (see [2, 3, 4]). The goal of my talk is to clarify the transition mechanism of pinning or depinning process of TPO. Our strategy is two-fold: HIOP (Heterogeneity-Induced-Ordered-Patterns) approach and a reduction method to a finite-dimensional system. HIOP is originally an object on the whole line and is defined by the set of all solution branches of ordered patterns caused by the heterogeneity such as unstable standing pulse pinned by its tail to the heterogeneity. Reduction method works quite well for localized patterns because of its particle characterization. Oscillatory nature of the tail is encoded in the existence of infinitely manny critical points in the phase space in the reduced ODE system.

6. Basin boundary experiences infinitely many reconnections

To answer the question when and how the transition occurs, we need to identify the basin boundary in the initial space and how it behaves as ε varies. It turns out that, for each fixed ε, the *basin boundary* separating two outputs can be characterized by the stable manifold of the saddle point relevant to the transition. The destination of time-reversal direction of this stable manifold is one of the critical points for each fixed ε and the location of this destination moves leftward toward $infty$ as $|\varepsilon|$ is increased so that reconnection occurs infinitely many times before reaching the transition point at which the pulse orbit coincides with the stable manifold. For further increase of $|\varepsilon|$, the pulse orbit becomes below the basin boundary and settles down to another asymptotic state.

7. Sensitive dependence on the initial condition and open questions

The fact that the basin boundary undergoes infinitely many reconnections successively among relevant critical points just before the transition is a key to understand the sensitive dependence of TPOs on the initial condition. In fact, suppose that the destination of the basin boundary is a critical point of spiral type, then it wraps around infinitely many times (in time-reversal direction) so that the final output becomes very sensitive to the choice of the initial data around the spiral critical point in any direction of ray. There still remain many open questions, in particular, for the dynamics in higher dimensional space. It is possible to reduce the PDE dynamics to 4D finite-dimensional system for two-dimensional space, however the basin boundary between two outputs becomes much more complicated than 1D case because the dimension of stable/unstable manifolds of critical points is increased and the interrelation among them is yet to be investigated. Moreover the geometry of heterogeneity affects a lot on the propagating behavior of spots. Nevertheless the analysis for 1D case here sheds a light on some aspect of the essential properties of the complicated dynamics of localized traveling patterns with oscillatory tails.

References

[1] Y. Nishiura and T. Watanabe, *Traveling pulses with oscillatory tails, figure-eight-like stack of isolas, and dynamics in heterogeneous media*, Preprint (2021).
[2] Y. Nishiura, T. Teramoto and K.-I. Ueda, *Dynamic transitions through scattors in dissipative systems*, Chaos **13**(3) (2003), 962–972.
[3] Y. Nishiura, T. Teramoto and K.-I. Ueda, *Scattering and separators in dissipative systems*, PRE **67**(5) (2003), 056210.
[4] Y. Nishiura, T. Teramoto and K.-I. Ueda, *Scattering of traveling spots in dissipative systems*, Chaos **15**(4) (2005), 047509.

Diffusive relaxation to equilibria for an extended reaction-diffusion system

Thierry Gallay
(joint work with Siniša Slijepčević)

We are interested in describing the long-time behavior of solutions to semilinear parabolic equations on unbounded spatial domains. A paradigmatic example is the Allen-Cahn equation

$$\partial_t u(x,t) \;=\; \Delta u(x,t) + u(x,t) - u(x,t)^3\,, \qquad x \in \mathbb{R}^N\,, \quad t > 0\,, \tag{1}$$

which is formally the L^2-gradient flow of the energy functional

$$E \;=\; \int_{\mathbb{R}^N} \Big(\frac{1}{2}\,|\nabla u|^2 + V(u)\Big)\,\mathrm{d}x\,, \qquad V(u) \;=\; \frac{1}{4}(1-u^2)^2\,.$$

The solutions we consider typically have infinite energy, so that we cannot use E as a Lyapunov function to prove that all trajectories of the system converge to the set of equilibria as $t \to +\infty$. Besides, equation (1) has traveling wave solutions which show that convergence to equilibria cannot hold in the uniform topology associated with the L^∞ norm. In what follows, we investigate the long-time behavior with respect to the (weaker) topology of uniform convergence on compact sets. Given a uniformly bounded solution $u(x,t)$ of (1), we thus define the ω-limit set

$$\omega \;=\; \Big\{\phi \in L^\infty(\mathbb{R}^N) \,\Big|\, \exists\, t_k \to \infty \text{ such that } u(\cdot,t_k) \xrightarrow[k\to\infty]{L^\infty_{\mathrm{loc}}} \phi\Big\}\,. \tag{2}$$

General arguments show that ω is non-empty and bounded in $L^\infty(\mathbb{R}^N)$, compact and connected in $L^\infty_{\mathrm{loc}}(\mathbb{R}^N)$, and fully invariant under the evolution defined by (1).

Following [10], we say that the solution u is *quasiconvergent* if ω is contained in the set of equilibria. As surprising as it may appear, quasiconvergence does not always hold, even for the solutions of the one-dimensional Allen-Cahn equation. A counter-example is given by the *coarsening dynamics* investigated in [3, 9].

The dissipative properties of infinite-energy solutions to (1) can be studied using the local energy balance

$$\partial_t e(t,x) \;=\; \mathrm{div}_x f(t,x) - d(t,x)\,, \tag{3}$$

where e is the energy density, f the energy flux, and d the energy dissipation rate. For the Allen-Cahn equation, one has

$$e \;=\; \frac{1}{2}|\nabla u|^2 + V(u)\,, \qquad f \;=\; (\partial_t u)\nabla u\,, \qquad d \;=\; (\partial_t u)^2\,,$$

so that $e \ge 0$, $d \ge 0$, and $|f|^2 \le Ced$ for some constant $C > 0$. Using these observations, we proved in a previous work [5] that, if $N = 1$ or 2, all bounded solutions of (1) on $\mathbb{R}^N$ converge in L^∞_{loc} to the set of equilibria for "almost all times" as $t \to +\infty$. In particular, the ω-limit set (2) always contains an equilibrium. Counter-examples indicate that these conclusions cannot be extended to higher space dimensions.

In the present talk, we consider reaction-diffusion systems associated with reversible chemical reactions of the form

$$\alpha_1\mathcal{A}_1 + \cdots + \alpha_n\mathcal{A}_n \;\underset{k'}{\overset{k}{\rightleftharpoons}}\; \beta_1\mathcal{A}_1 + \cdots + \beta_n\mathcal{A}_n\,,$$

where $\mathcal{A}_1,\dots,\mathcal{A}_n$ denote the reactant and product species, $k, k' > 0$ are the reaction rates, and the nonnegative integers α_i, β_i $(i = 1,\dots,n)$ are the stoichiometric coefficients. According to the law of mass action, the concentration $c_i(x,t)$ of the species $\mathcal{A}_i$ satisfies the reaction-diffusion equation

$$\partial_t c_i \;=\; d_i\Delta c_i + (\beta_i - \alpha_i)\Biggl(k\prod_{j=1}^n c_j^{\alpha_j} - k'\prod_{j=1}^n c_j^{\beta_j}\Biggr)\,, \qquad i = 1,\dots,n\,, \tag{4}$$

where $d_i > 0$ denotes the diffusion coefficient of species $\mathcal{A}_i$, see [7]. It happens that positive solutions of (4) satisfy the entropy balance (3) with

$$e(x,t) \;=\; \sum_{i=1}^n \phi\bigl(c_i(x,t)\bigr)\,, \qquad f(x,t) \;=\; \sum_{i=1}^n d_i \log(c_i(x,t))\nabla c_i(x,t)\,,$$

$$d(x,t) \;=\; \sum_{i=1}^n d_i\frac{|\nabla c_i(x,t)|^2}{c_i(x,t)} + k\log\biggl(\frac{B(x,t)}{A(x,t)}\biggr)\Bigl(B(x,t) - A(x,t)\Bigr)\,,$$

where $\phi(z) = z\log(z) - z + 1$ and $A(x) = \prod c_j(x)^{\alpha_j}$, $B(x) = \prod c_j(x)^{\beta_j}$. This gradient structure can be used to prove that all solutions of system (4) in a bounded domain of $\mathbb{R}^N$ converge to the global chemical equilibrium as $t \to +\infty$ [1, 2, 4, 8].

To explore what happens in unbounded domains, we concentrate here on the simple particular case

$$(5)\qquad \begin{aligned} u_t(x,t) &= a u_{xx}(x,t) + v(x,t)^2 - u(x,t)\,, & x \in \mathbb{R}\,,\\ v_t(x,t) &= b v_{xx}(x,t) + 2\big(u(x,t) - v(x,t)^2\big)\,, & t > 0\,, \end{aligned}$$

which corresponds to the (simplistic) reaction $\mathcal{A} \rightleftharpoons 2\mathcal{B}$ with rates $k = k' = 1$. The parameters are the diffusion constants $a, b, > 0$, and a rescaling shows that the ratio a/b is the only relevant quantity. It is easy to verify that system (5) is globally well-posed for nonnegative initial data $(u_0, v_0) \in L^\infty(\mathbb{R})^2$, and that the corresponding solution satisfies the uniform bound

$$2\|u(\cdot,t)\|_{L^\infty} + \|v(\cdot,t)\|_{L^\infty} \le 2\|u_0\|_{L^\infty} + \|v_0\|_{L^\infty}\,, \qquad \forall\, t \ge 0\,.$$

Our main result [6] shows that this solution converges to the manifold of local chemical equilibria as $t \to +\infty$.

Proposition. *The solution of* (5) *with nonnegative initial data* $(u_0, v_0) \in L^\infty(\mathbb{R})^2$ *satisfies, for all* $t > 0$,

$$\|u_x(\cdot,t)\|_{L^\infty} + \|v_x(\cdot,t)\|_{L^\infty} \le \frac{C}{t^{1/2}}\log(2+t)\,, \quad \|u(\cdot,t) - v(\cdot,t)^2\|_{L^\infty} \le \frac{C}{(1+t)^{1/2}}\,,$$

where the constant only depends on the parameters a, b *and on* $\|u_0\|_{L^\infty}, \|v_0\|_{L^\infty}$.

The proof is quite simple in the case of equal diffusivities $a = b$, because the quantity $w = 2u + v$ then satisfies the linear heat equation $w_t = a w_{xx}$. In the general case, our argument relies on the local energy balance $e_t = f_x - d$ where

$$e = \frac{1}{2}u^2 + \frac{1}{6}v^3\,, \qquad f = a u u_x + \frac{b}{2}v^2 v_x\,, \qquad d = a u_x^2 + b v v_x^2 + \rho^2\,,$$

where the quantity $\rho = u - v^2$ measures the distance to the local chemical equilibrium. We also exploit the higher-order balance $\tilde{e}_t = \tilde{f}_x - \tilde{d}$, where

$$\begin{aligned} \tilde{e} &= \frac{a+b}{2}u_x^2 + b\,v v_x^2 + \frac{1}{2}\rho^2\,,\\ \tilde{f} &= (a+b)u_x u_t + 2b\,v v_x v_t - \frac{b^2}{3}v_x^3 + b\,\rho\rho_x\,,\\ \tilde{d} &= a(a+b)u_{xx}^2 + 2b^2 v v_{xx}^2 + (1+4v)\rho^2 + b\,\rho_x^2 - 2a\rho u_{xx} + 4b\rho v v_{xx}\,. \end{aligned}$$

It is important here to note that $\tilde{d} \ge 0$ and that $\tilde{e} \le Cd$ for some constant $C > 0$. The existence of such an ordered pair of dissipative structures allows us to go beyond the general conclusions of [5] and to prove convergence to equilibria for *all times*, thus precluding in particular any coarsening-like dynamics. Whether or not such an approach can be extended to more general reaction-diffusion systems of the form (4) is the object of current investigation.

References

[1] L. Desvillettes and K. Fellner, *Exponential decay toward equilibrium via entropy methods for reaction-diffusion equations*, J. Math. Anal. Appl. **319** (2006), 157–176.

[2] L. Desvillettes, K. Fellner, and Bao Quoc Tang, *Trend to equilibrium for reaction-diffusion systems arising from complex balanced chemical reaction networks*, SIAM J. Math. Anal. **49** (2017), 2666–2709.

[3] J.-P. Eckmann and J. Rougemont, *Coarsening by Ginzburg-Landau dynamics*, Comm. Math. Phys. **199** (1998), 441–470.

[4] K. Fellner and Bao Quoc Tang, *Explicit exponential convergence to equilibrium for nonlinear reaction-diffusion systems with detailed balance condition*, Nonlinear Analysis **159** (2017), 145–180.

[5] Th. Gallay and S. Slijepčević, *Distribution of energy and convergence to equilibria in extended dissipative systems*, J. Dynam. Differential Equations **27** (2015), 653–682.

[6] Th. Gallay and S. Slijepčević, *Diffusive relaxation to equilibria for an extended reaction-diffusion system on the real line*, preprint arXiv:2106.15137 (2021).

[7] F. Horn and R. Jackson, *General mass action kinetics*, Arch. Rational Mech. Anal. **47** (1972), 81–116.

[8] A. Mielke, *Uniform exponential decay for reaction-diffusion systems with complex-balanced mass-action kinetics*, Patterns of dynamics, 149–171, Springer Proc. Math. Stat. **205**, Springer, Cham, 2017.

[9] P. Poláčik, *Examples of bounded solutions with nonstationary limit profiles for semilinear heat equations on* $\mathbb{R}$, J. Evol. Equ. **15** (2015), 281–307.

[10] P. Poláčik, *Convergence and quasiconvergence properties of solutions of parabolic equations on the real line: an overview*, In "Patterns of Dynamics", pp. 172–183, Springer Proc. Math. Stat. **205**, Springer, Cham, 2017.

Stability of smooth periodic traveling waves in the Camassa-Holm equation

Anna Geyer

(joint work with Renan H. Martins, Fábio Natali, Dmitry E. Pelinovsky)

We solve the open problem of spectral stability of smooth periodic waves in the Camassa–Holm equation,

$$u_t - u_{txx} + 3uu_x = 2u_x u_{xx} + uu_{xxx} \tag{1}$$

which was derived in [1, 2] and justified in [4, 6] as a model for the propagation of unidirectional shallow water waves. The key to obtaining this stability result is that the periodic waves of the Camassa–Holm equation can be characterized by an alternative Hamiltonian structure,

$$\frac{dm}{dt} = J_m \frac{\delta E}{\delta m}, \quad J_m = -\left(m\partial_x + \partial_x m\right), \quad \frac{\delta E}{\delta m} = u, \tag{2}$$

where $m := u - u_{xx}$ and

$$E(m) = \frac{1}{2}\int_0^L (u_x^2 + u^2)dx, \tag{3}$$

which is different from the standard formulation common to the Korteweg-de Vries equation. The standard formulation has the disadvantage that the period function is not monotone [5], and the quadratic energy form may have two rather than one negative eigenvalues. We prove that the nonstandard formulation has the advantage that the period function is monotone using a criterion by Chicone [3], and the quadratic energy form has only one simple negative eigenvalue. We deduce a precise condition for the spectral and orbital stability of the smooth periodic travelling waves and show numerically that this condition is satisfied in the open region where the smooth periodic waves exist.

References

[1] R. Camassa and D.D. Holm, "An integrable shallow water equation with peaked solitons", *Phys. Rev. Lett.* **71** (1993), 1661–1664.

[2] R. Camassa, D. Holm, and J. Hyman, "A new integrable shallow water equation", *Adv. Appl. Math.* **31** (1994), 1–33.

[3] C. Chicone, "The monotonicity of the period function for planar Hamiltonian vector fields", *J. Diff. Equat.* **69** (1987), 310–321.

[4] A. Constantin and D. Lannes, "The hydrodynamical relevance of the Camassa–Holm and Degasperis–Procesi equations", *Arch. Ration. Mech. Anal.* **192** (2009), 165–186.

[5] A. Geyer and J. Villadelprat, "On the wave length of smooth periodic traveling waves of the Camassa–Holm equation", *J. Diff. Equat.* **259** (2015), 2317–2332.

[6] R.S. Johnson, "Camassa–Holm, Korteweg–de Vries and related models for water waves", *J. Fluid Mech.* **455** (2002), 63–82.

Noninvasive control of singular patterns

Frits Veerman

Noninvasive (Pyragas) control aims to control the stability of special solutions such as periodic orbits, in general n-dimensional dynamical systems by adding a control term g that vanishes on the 'target' solution - hence the term 'noninvasive' - but has a nontrivial (local) structure in the neighbourhood of the target solution, thereby influencing its stability properties. Hence, a suitable choice of the control term can stabilize the target solution. This approach can also be applied to infinite-dimensional dynamical systems, such as reaction-diffusion systems, where stationary patterns are obvious candidates for 'special solutions' to be stabilized. For a wide range of patterns in (scalar) reaction-diffusion equations, Isabelle Schneider (FU Berlin) has shown that a well-chosen combination of spatio-temporal delay can stabilize said patterns. We show that the techniques and ideas developed in this scalar setting can be extended to a class of singularly perturbed reaction diffusion systems, where scale separation plays a key role in the (constructive) existence and stability analysis of so-called singular patterns. Incorporating different strategies (proportional, time-developed) in the existing Evans function framework, our preliminary results show that single homoclinic singular pulses can always be stabilized using proportional control, while the efficacy of time-developed feedback depends on the structure of the pulse spectrum.

Spectral stability of pattern-forming fronts in the complex Ginzburg-Landau equation with a quenching mechanism

Björn de Rijk
(joint work with Ryan Goh)

We consider the stability of pattern-forming fronts invading a destabilized ground state. In spatially homogeneous systems stability of such fronts can only be obtained in exponentially weighted spaces as any perturbation ahead of the front grows exponentially in time due to the instability of the ground state. On the other hand, pattern-forming fronts are observed in various spatially inhomogeneous settings such as light-sensing reaction-diffusion systems, directional solidification of crystals or ion beam milling. In these settings the unstable state is only established in the wake of the progressing heterogeneity after which patterns start to nucleate. Consequently, perturbations cannot grow far ahead of the interface of the pattern-forming front. This begs the question of whether stability of these quenched fronts can be rigorously established in more natural spaces. In this talk we present a first step towards answering this question affirmative by showing the spectral stability of pattern-forming fronts against L^2-perturbations in the spatially inhomogeneous complex Ginzburg-Landau (cGL) equation

$$(1) \qquad A_t = (1 + \mathrm{i}\alpha)A_{xx} + \chi(x - ct)A - (1 + \mathrm{i}\gamma)A|A|^2, \qquad A \in \mathbb{C},\, x, t \in \mathbb{R},$$

posed in one space dimension, with dispersion parameters $\alpha, \gamma \in \mathbb{R}$, and where $\chi\colon \mathbb{R} \to \mathbb{R}$, $\chi(\xi) = -\mathrm{sgn}(\xi)$ is a step-function heterogeneity, traveling with fixed speed $c \in \mathbb{R}$.

Pattern-forming fronts of the form $A(x, t) = \mathrm{e}^{\mathrm{i}\omega t}A_{\mathrm{tf}}(x - ct)$ in (1) have been obtained in the regime where the heterogeneity propagates with speed c just below the linear invasion speed c_{lin} of the base state, see [3]. Here, $\omega \in \mathbb{R}$ denotes the temporal frequency, and $A_{\mathrm{tf}}(\xi)$ is the profile function of the front connecting a periodic wave train at $-\infty$ to the base state $A \equiv 0$ at $+\infty$. As the free front solving the associated homogeneous problem with $\chi \equiv 1$ is pulled (i.e. it propagates with speed c_{lin}), the quenched front locks to the interface of the heterogeneity leaving a long intermediate state of length $\mathcal{O}(1/\sqrt{c_{\mathrm{lin}} - c})$ lying near the unstable base state. This manifests itself in the spectrum of the linearization of (1) about the front through the accumulation of eigenvalues onto the absolute spectrum associated with the unstable base state, cf. [8]. As $c \uparrow c_{\mathrm{lin}}$ the absolute spectrum stabilizes with the same rate at which eigenvalues accumulate onto it allowing us to rigorously establish spectral stability of the front. That is, the spectrum is confined to the left-half plane and touches the imaginary axis only at the origin as a parabolic curve reflecting the diffusive stability of the periodic wave train at $-\infty$. In addition, an embedded eigenvalue resides at the origin due to gauge symmetry. On the other hand, we note that there is no translational eigenvalue at the origin due to the spatial inhomogeneity in (1).

The presence of unstable absolute spectrum poses a technical challenge as spatial eigenvalues along the intermediate state no longer admit a hyperbolic splitting and standard tools such as exponential dichotomies are unavailable. Instead, we projectivize the linear flow as in [7] and study the associated matrix Riccati equation describing the dynamics of subspaces on the Grassmannian manifold using the superposition principle [6], Riemann surface unfolding and the Möbius transform. Eigenvalues can then be identified as the roots of the meromorphic Riccati-Evans function [5], and can be located using winding number and parity arguments.

To our knowledge, this is the first rigorous result considering the spectral stability of quenched pattern-forming fronts. Thereby, it is the important first step towards addressing nonlinear stability of such fronts. To establish nonlinear stability of the spectrally stable pattern-forming front in (1) one could try to proceed as in [1], where, under similar spectral conditions, nonlinear stability of source defects in the homogeneous cGL equation has been obtained.

We expect our spectral analysis to be prototypical in the sense that similar mechanisms (i.e. the same subtle dance between accumulating point spectrum and stabilizing weakly unstable absolute spectrum) will govern the stability of pattern-forming fronts in other important spatially inhomogeneous models, such as the Swift-Hohenberg equation, the Cahn-Hilliard equation, and certain reaction-diffusion systems, where the free invasion front in the associated homogeneous equation is pulled. However, in such models, periodic patterns are generally not relative equilibria under the action of a gauge symmetry as in (1) so temporal dynamics cannot be factored out and pattern-forming front solutions are modulated traveling waves. This means the associated eigenvalue problem, as well as the nonlinear existence problem, are infinite-dimensional. One would hope to perform a center-manifold analysis to reduce the eigenvalue problem down to a finite-dimensional ODE system whose dynamics resemble the system considered in this work.

A further subject of future research is to consider the case, where the free invasion front in the associated spatially homogeneous equation is not pulled, but pushed, i.e. due to nonlinear effects the free front spreads at a speed $c_{\mathrm{p}} > c_{\mathrm{lin}}$. Thus, one expects no absolute unstable intermediate state. In fact, preliminary simulations [2] indicate that stability is governed by a single fold eigenvalue, reminiscent of snaking phenomena. A starting point would be to consider the spatially inhomogeneous cubic-quintic Ginzburg-Landau equation, where pattern-forming fronts have been obtained in [4] for wave speeds $c \approx c_{\mathrm{p}}$. We anticipate that the relative position of the oscillatory eigenvalue with respect to the origin, which dictates the stability of the pattern-forming front, could be rigorously tracked using parity arguments with the Riccati-Evans function as in the current analysis.

References

[1] M. Beck, T. T. Nguyen, B. Sandstede, K. Zumbrun, *Nonlinear stability of source defects in the complex Ginzburg-Landau equation*, Nonlinearity **27**(4) (2014), 739–786.

[2] R. Goh, B. de Rijk, *Spectral stability of pattern-forming fronts in the complex Ginzburg-Landau equation with a quenching mechanism*, arXiv:2006.15083 (2020).

[3] R. Goh, A. Scheel, *Triggered fronts in the complex Ginzburg Landau equation*, J. Nonlinear Sci. **24**(1) (2014), 117–144.

[4] R. Goh, A. Scheel, *Pattern formation in the wake of triggered pushed fronts*, Nonlinearity **29**(8) (2016), 2196–2237.

[5] K. E. Harley, P. van Heijster, R. Marangell, G. J. Pettet, M. Wechselberger, *Numerical computation of an Evans function for travelling waves*, Mathematical Biosciences **266** (2015), 36–51.

[6] J. Harnad, P. Winternitz, R. L. Anderson, *Superposition principles for matrix Riccati equations*, J. Math. Phys. **24**(5) (1983), 1062–1072.

[7] V. Ledoux, S. J. A. Malham, J. Niesen, V. Thümmler, *Computing stability of multidimensional traveling waves*, SIAM J. Appl. Dyn. Syst. **8**(1) (2009), 480–507.

[8] B. Sandstede, A. Scheel, *Absolute and convective instabilities of waves on unbounded and large bounded domains*, Phys. D **145**(3-4) (2000), 233–277.

Existence of Spiral Waves in Oscillatory Media with Nonlocal Coupling

Gabriela Jaramillo

Systems that can be classified as oscillatory media consist of small oscillating elements that interact with each other via some form of coupling. In this talk we will be particularly interested in systems where these interactions are assumed to be nonlocal. As an example, we consider oscillating chemical reactions that include a fast component which can be eliminated adiabatically. Consequently, these reactions can be modeled using integro-differential equations.

Our interest in these systems comes from numerical experiments performed by Kuramoto and coauthors, which showed that the nonlocal interactions are responsible for creating new patterns called chimera spirals, [4, 6]. These patterns resemble an archimedian spiral in the far field, but have a core that is not oscillating in synchrony with the rest of the pattern. Understanding why and how these structure arise provides the motivation for this project. As a first step in this direction we revisit the existence of spiral waves in the context of oscillatory systems with nonlocal coupling.

To carry out the analysis we consider an abstract system of integro-differential equations,

$$U_t = K * U + F(U;\lambda) \quad U \in \mathbb{R}^2 \quad x = (r,\theta) \in \mathbb{R}^2, \quad \lambda \in \mathbb{R}$$

with nonlinearities, $F(U;\lambda)$ that undergo a Hopf bifurcation when $\lambda = 0$. For simplicity, we concentrate on the particular case of kernels that have Fourier symbols of the form, $\hat{K}(\xi) = -\sigma|\xi|^2/(1 + D|\xi|^2)$, with $\xi \in \mathbb{R}^2$.

To prove the existence of spiral waves, we first derive an amplitude equation which governs the dynamics of rotating wave solutions. We then proceed to prove the existence of these patterns using this reduced equation. Notice that because we work with convolution operators, we can no longer use tools from spatial dynamics to derive a normal form, as is done in [5]. Instead, we use the method of multiple scales, which assumes that the solution can be written as a regular expansion in powers of $\varepsilon \sim \sqrt{\lambda}$. Therefore, we also have to prove that this expansion converges, or equivalent, that the amplitude equation provides valid approximations to the solutions of the original system.

Because our solutions are periodic in time, we can combine these two steps, deriving the amplitude equation and proving its validity, using a similar method to

Lyapunov-Schmidt reduction. This approach consists on carrying out the standard multiple scale analysis, giving us a hierarchy of equations at different powers of ε. As is standard, the first and second order equations can easily be solved. However, in contrast to the traditional method where one derives the amplitude equation at cubic order as a solvability condition, we gather all cubic and higher order terms in one equation, which we further split as follows,

$$L_{\|}U_3 = PN(U_1, U_3; \varepsilon, \mu), \tag{1}$$

$$L_{\perp}U_3 = (1-P)N(U_1, U_3; \varepsilon, \mu). \tag{2}$$

The key idea is that one can pick Banach spaces, X, Y and a projection, $P : X \to X_{\|}$, in such a way that the operator L can be split into an invertible operator, $L_{\perp} : X_{\perp} \to Y_{\perp}$, and a bounded operator, $L_{\|} : X_{\|} \to Y_{\|}$. One can then use equation (2) to solve for the variable U_3 in terms of U_1 via the implicit function theorem. Inserting the result into equation (1), and assuming that U_3 does not have a component in the direction of $X_{\|}$, then gives the amplitude equation

$$\tilde{K}_{\varepsilon,n} * w + \lambda w + \alpha |w|^2 w + \mathrm{O}(\varepsilon |w|^4 w) = 0. \tag{3}$$

We point out three features of the above equation. 1) The convolution kernel $\tilde{K}_{\varepsilon,n}$ represents a rescaling of K. 2) The imaginary part of λ is related to the rotational speed of the wave and is a free parameter that needs to be determined when solving the equation. 3) To be able to say that solutions to the amplitude equation provide good approximations to the solutions of the original system, one has to solve the full equation and include all higher order terms.

We now briefly explain our current efforts for proving the existence of spiral waves in the supercritical case, i.e $\lambda_R > 0$ and $\alpha_R < 0$. As above, we use methods from functional analysis to accomplish this. Because formally $K \sim (1+D\Delta)^{-1}\sigma\Delta$, we may precondition (3) with $(1 + D\Delta)$, and arrive at an equation that resembles the complex Ginzburg-Landau equation (cGL),

$$\beta\Delta_n * w + \lambda w + \alpha |w|^2 w + \tilde{N}(w, \varepsilon) = 0, \qquad \beta = (\sigma - \varepsilon^2 D\lambda_R) - \mathrm{i}(\varepsilon^2 D\lambda_I).$$

We can then apply a multiple scale analysis using the same scalings that are typical for deriving the phase dynamics approximation of the cGL, see [1]. As above, this is then combined with a modified Lyapunov-Schmidt reduction to close the argument and prove existence of solutions. The result is once a gain a hierarchy of equations, with the first equation encapsulating information about the amplitude of the pattern, and the second equation describing the dynamics of the phase. Interestingly, we find that the phase dynamics is govern by a viscous eikonal equation with an inhomogeneity that is a function of the zeroth-order approximation to the amplitude. This equation is known to provide a model for the emergence of target patterns in oscillatory media, and has been solved in [2]. Since in the current context, these particular solutions correspond to spiral waves, we can adapt the results form [2] and derive an approximation for the wavenumber of spiral waves patterns.

We have two cases. If $\sigma - \varepsilon^2 \lambda_R D > 0$, then the wavenumber is well approximated by $k(\varepsilon) \sim \frac{2e^{-\gamma_e}}{|b|} \exp(1/a)$ with $a = \varepsilon a_1 + \varepsilon^2 a_2 + O(\varepsilon^3)$ and

$$a_1 \sim \frac{\sigma - \varepsilon^2 \lambda_R D}{\lambda_R} \left(\frac{\alpha_I}{\alpha_R} \right)^2 \qquad b \sim -\frac{\alpha_I}{\alpha_R}.$$

On the other hand, if $\sigma - \varepsilon^2 \lambda_R D < 0$, then $k(\varepsilon) \sim \frac{2e^{-\gamma_e}}{|b|} \exp(-1/a)$ with $a = \varepsilon a_1 + \varepsilon^2 a_2 + O(\varepsilon^3)$ and

$$a_1 =\sim \frac{\sigma - \varepsilon^2 \lambda_R D}{\lambda_R} \left(\frac{\alpha_I}{\alpha_R} \right)^2 \qquad b \sim -\frac{\alpha_I}{\alpha_R}.$$

The above results are obtained by matching intermediate and far field approximations for the phase. This process also selects the value of the free parameter λ_I. Figure 1 shows that these results are in qualitative agreement with our numerical simulations. Notice that for the specified parameter values, the patterns found correspond to spiral chimeras. Thus, with the method presented here we are able to prove existence of spiral waves and spiral chimeras at the same time. However, with our current set up we are not able to distinguish between these two patterns. We plan to address this in future work.

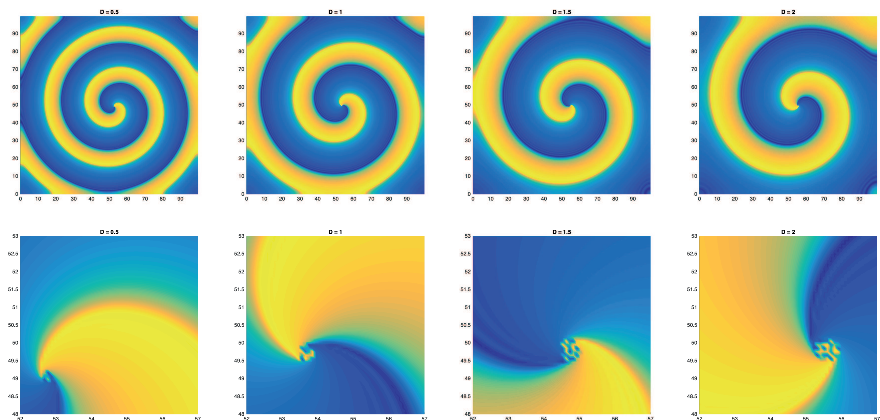

FIGURE 1. Simulations of a FH-N system with nonlocal coupling described by $\hat{K}(\xi) = -\sigma|\xi|^2/(1 + D|\xi|^2)$. All parameters fixed with $\sigma = 0.1$. Pictures correspond to different values of $D = 0.5, 1.0, 1.5, 2.0$. For these parameter values our patterns represent spiral chimeras.

References

[1] A. Doelman, et al. *The dynamics of modulated wave trains,* American Mathematical Soc., 2009.

[2] G. Jaramillo, Gabriela, S. C. Venkataramani, *Target patterns in a 2D array of oscillators with nonlocal coupling,* Nonlinearity 31.9 (2018): 4162.

[3] G. Jaramillo, *Rotating waves in oscillatory media with nonlocal interactions and their normal form,* arXiv preprint arXiv:2103.14940 (2021).
[4] Y. Kuramoto, and D. Battogtokh, *Coexistence of Coherence and Incoherence in Nonlocally Coupled Phase Oscillators,* Nonlinear Phenomena in Complex Systems 5.4 (2002): 380-385.
[5] A. Scheel, *Bifurcation to spiral waves in reaction-diffusion systems,* SIAM journal on mathematical analysis 29.6 (1998): 1399-1418.
[6] S. Shima, and Y. Kuramoto, *Rotating spiral waves with phase-randomized core in nonlocally coupled oscillators,* Physical Review E 69.3 (2004): 036213.

Oscillatory integrators for the Klein–Gordon equation and related systems

Katharina Schratz
(joint work with María Cabrera Calvo)

A novel class of oscillatory low regularity uniformly accurate integrators was recently introduced in [3] for the Klein–Gordon equation

$$
\begin{aligned}
c^{-2}\partial_{tt}z(t,x) - \Delta z(t,x) + c^2 z(t,x) &= |z(t,x)|^2 z(t,x),\\
z(0,x) &= z_0(x), \qquad (1)\\
\partial_t z(0,x) &= c^2 z_0'(x).
\end{aligned}
$$

This work allowed us to close the gap between the general low regularity framework introduced in [4] for a class of abstract evolution equations, and the uniformly accurate approach for highly oscillatory problems with oscillations $e^{ic^2\ell t}$ presented in [1]. Indeed, the leading operator in (1) has the form

$$\langle\nabla\rangle_c^2 = c^2 - \Delta$$

with the full spectrum of low to high frequencies (e.g., in the periodic case $(\Delta)_k = -k^2$) coupled with a possibly large parameter c. The underlying oscillations

$$\sum_\ell e^{ic\langle\nabla\rangle_c \ell t}$$

are numerically delicate to tackle, in particular, in non relativistic regimes where $c \gg 1$. The idea of the new class of methods derived in [3] lies in embedding the dominant oscillations explicitly into the numerical scheme while only approximating the non oscillatory parts. The latter allows for approximation results that hold uniformly in c while requiring less regularity than pre-existing methods. In order to achieve this, in a first step we express (1) as a first order system. Setting

$$u = z - ic^{-1}\langle\nabla\rangle_c^{-1}\partial_t z, \quad v = z - ic^{-1}\langle\nabla\rangle_c^{-1}\partial_t \overline{z}, \qquad (2)$$

a simple calculation shows that $z = \frac{1}{2}(u + v)$. Furthermore, if we assume that $z(t,x) \in \mathbb{R}$, we have $v \equiv u$.

A short calculation shows that the corresponding first order system in u reads

$$i\partial_t u + c\langle\nabla\rangle_c u - \frac{1}{8}c\langle\nabla\rangle_c^{-1}\big(u + \overline{u}\big)^3 = 0, \quad u(0) = z(0) - ic^{-1}\langle\nabla\rangle_c^{-1}\partial_t z(0). \qquad (3)$$

Embedding the dominant oscillations in the iteration of Duhamel's formula of (3) into the numerical discretisation leads to the first order low regularity uniformly accurate scheme ([3])

$$\begin{aligned} u^{n+1} &= e^{i\tau c\langle\nabla\rangle_c}u^n - i\tau\frac{1}{8}c\langle\nabla\rangle_c^{-1}e^{i\tau c\langle\nabla\rangle_c}\big[3\big(u^n\big)^2\varphi_1(-2i\tau(c\langle\nabla\rangle_c - c^2))\overline{u^n} \\ &\quad + \varphi_1(-2i\tau(c\langle\nabla\rangle_c + c^2))\big(\overline{u^n}\big)^3 + 3u^n\varphi_1(-2i\tau c\langle\nabla\rangle_c)\big(\overline{u^n}\big)^2\varphi_1(2ic^2\tau)\big(u^n\big)^3\big], \end{aligned}$$

with

$$\varphi_1(z) = \frac{e^z - 1}{z}.$$

A natural question is how one can extend this idea of low regularity approximations coupled with uniform accuracy to a more general class of Klein–Gordon type systems, for example coupled Klein–Gordon equations or Klein–Gordon–Schrödinger systems. Let us consider for instance

$$\begin{aligned} c_1^{-2}\partial_{tt}z_1(t,x) - \Delta z_1(t,x) + c_1^2 z_1(t,x) &= |z_2(t,x)|^2, \\ c_2^{-2}\partial_{tt}z_2(t,x) - \Delta z_2(t,x) + c_2^2 z_2(t,x) &= |z_1(t,x)|^2, \\ (z_1, \partial_t z_1)(t=0) &= (z_1^0, c_1^2 z_1^1), \\ (z_2, \partial_t z_2)(t=0) &= (z_2^0, c_2^2 z_2^1). \end{aligned} \tag{4}$$

Similarly, via (2), we may express (4) as a coupled first order system in u_1, u_2. Taylor series expansion of the function $x \mapsto \sqrt{1+x^2}$ gives

$$c\langle\nabla\rangle_c = c^2 - \frac{1}{2}\Delta + \mathcal{O}\bigg(\frac{\Delta^{\alpha+1}}{c^{2\alpha}}\bigg), \quad 0 \le \alpha \le 1. \tag{5}$$

This allows the following expansion of the underlying oscillations

$$e^{-isc_1\langle\nabla\rangle_{c_1}}e^{isc_2\langle\nabla\rangle_{c_2}} = e^{-is(c_1^2 - c_2^2)} + \mathcal{O}\bigg(\frac{\Delta^2}{\min\{c_1^2, c_2^2\}}\bigg). \tag{6}$$

Hence, the oscillations only cancel if $c_1 = c_2$ holds, and otherwise smooth solutions are required.

Observation (6) implies that the techniques in [3] are restricted to the case where we have equal velocity in our system. The same problem arises in the case of Klein–Gordon–Schrödinger systems, where the central oscillations take the form

$$\sum_{\ell} e^{-is(c\langle\nabla\rangle_c + \ell\Delta)}$$

which, similarly to (4) can not be handled with the proposed techniques in [3] either, or only by requiring the classical regularity H^{r+2}, $r > \frac{d}{2}$ of pre-existing methods (see, for instance, [2]).

These are open problems and will require novel filtering, cutoff and Fourier techniques.

References

[1] S. Baumstark, E. Faou, K. Schratz, *Uniformly accurate oscillatory integrators for Klein-Gordon equations with asymptotic convergence to the classical NLS splitting*, Math. Comp. 87:1227–1254 (2018)

[2] S. Baumstark, G. Kokkala, K. Schratz, *Asymptotic consistent exponential-type integrators for Klein-Gordon-Schrödinger systems from relativistic to non-relativistic regimes*, ETNA 48:63-80 (2018)

[3] M. Cabrera Calvo, and K. Schratz, *"Uniformly accurate low regularity integrators for the Klein–Gordon equation from the classical to non-relativistic limit regime"*,https://arxiv.org/abs/2104.11672

[4] F. Rousset, K. Schratz, *A general framework of low regularity integrators*, to appear in SIAM J. Numer. Anal., http://arxiv.org/abs/2010.01640

Noisy Waves

Hermen Jan Hupkes

(joint work with C.H.S. Hamster)

We discuss techniques to establish the stability of stochastically forced waves on timescales that are exponentially long with respect to the noise-strength, for a general class of reaction-diffusion systems that includes the Nagumo and (diffusive) FitzHugh-Nagumo problems. We point out connections with deterministic existence and stability analysis that can be used to uncover the stochastic corrections to the speed and shape of the waveprofiles. This talk is based on results contained in the papers [1, 2, 3, 4]. For an excellent review on the broad topic of stochastically forced waves we refer to [5].

References

[1] C. H. S. Hamster and H. J. Hupkes (2020), Stability of Travelling Waves on Exponentially Long Timescales in Stochastic Reaction-Diffusion Equations. *SIAM Journal on Applied Dynamical Systems* **19**(4), 2469–2499.

[2] C. H. S. Hamster and H. J. Hupkes (2020), Stability of Traveling Waves for Systems of Reaction-Diffusion Equations with Multiplicative Noise. *SIAM Journal on Mathematical Analysis* **52**(2), 1386–1426.

[3] C. H. S. Hamster and H. J. Hupkes (2019), Stability of Traveling Waves for Reaction-Diffusion Equations with Multiplicative Noise. *SIAM Journal on Applied Dynamical Systems* **18**(1), 205–278.

[4] C. H. S. Hamster and H. J. Hupkes (2020), Travelling waves for reaction–diffusion equations forced by translation invariant noise. *Physica D: Nonlinear Phenomena* **401**, 132233.

[5] C. Kuehn (2020), Travelling Waves in Monostable and Bistable Stochastic Partial Differential Equations. *Jahresbericht der Deutschen Mathematiker-Vereinigung* **122**(2), 73–107.

Rigorous validated numerics for the study of patterns in the Phase-Field-Crystal model

Jean-Philippe Lessard
(joint work with Rustum Choksi and Gabriel Martine La Boissonière)

Most metals, ceramics, and minerals are *polycrystalline* containing crystallines (grains) of different crystal orientation. The properties of the grain boundaries are of paramount importance for the macroscopic properties of the material (fracture, yield stress, coercivity, conductivity). Studying grain boundaries is an active field both in materials science and in applied mathematics (e.g. Mullins model and curvature driven motion).

In an attempt to model elasticity in polycrystals and grain growth, the Phase-Field-Crystal (PFC) model was proposed in 2002 in [1]. In this project, we consider the simplest two-dimensional model with in mind the study of thin films. Let Ω be a rectangle in $\mathbb{R}^2$ with periodic boundary conditions and consider $\psi \in H^2(\Omega)$ satisfying the *phase constraint* $\frac{1}{|\Omega|}\int_\Omega \psi = \bar{\psi}$. The *PFC energy* of ψ is defined as

$$E[\psi] = \frac{1}{|\Omega|}\int_\Omega \frac{1}{2}\left((\nabla^2 + q_0^2)\psi\right)^2 + \frac{1}{4}\left(\psi^2 - \beta\right)^2.$$

Its associated conservative H^{-1} gradient flow is known as the *PFC equation*

$$\psi_t = \nabla^2\left(\left(\nabla^2 + q_0^2\right)^2 \psi + \psi^3 - \beta\psi\right). \tag{1}$$

The fixed parameter q_0 sets the atomic distance $1/q_0$, while the active parameters are β (inversely proportional to temperature), the phase fraction $\bar{\psi}$ and the size of Ω. It is worth mentioning that the PFC model can also be derived from Density Functional Theory (DFT) by keeping only the closest neighbour correlations [2], which in this case models the *close-packing problem*. Moreover, it was shown in [3] that grain size distribution of late time PFC have a remarkable agreement with experimental data from aluminum thin films. This agreement extends to certain other geometric metrics, including perimeter.

While existence of solutions of (1) follows from Direct Methods, getting any rigorous statement about existence of nontrivial critical points and local minimizers is far from reach using standard PDE/variational methods. In fact, except for constant (liquid) state, it is very difficult to obtain rigorous results with such methods (e.g. see [4]). This is where the field of rigorously validated numerics provides a new tool. The goal of this project is to develop a general *computer-assisted* approach to prove (constructively) existence of nontrivial steady states in the 2D PFC model.

Let $\Omega = [0, L_x] \times [0, L_y]$ with $L_x = \frac{4\pi}{\sqrt{3}}N_x$ and $L_y = 4\pi N_y$, where $N_x, N_y \in \mathbb{N}$ are the number of atoms lined up in the x, y-axes. The main parameters of the problem are then $(\bar{\psi}, \beta)$ and the domain size is given by (N_x, N_y). In order to break the translational and rotational symmetries of PFC, we impose Neumann boundary conditions. Let a_α be the Fourier coefficients of ψ and let $(a_\alpha)_t$ be the time derivative. Inserting this expansion into the PFC equation results in an infinite system of equations of the form $(a_\alpha)_t = F_\alpha(a)$ thanks to orthogonality. The steady states may then be found numerically by solving $F(a) = 0$ up to some truncation order. The field of *rigorous numerics in dynamics* (e.g. see [5]) provides a machinery to prove existence of true zeroes of F close to numerical approximations. This is done by showing (via functional analytic estimates and interval arithmetic computations) that a certain Newton-like operator is a contraction on a ball centered at the approximation. The contraction mapping theorem yields the wanted *true* steady state. We applied this machinery (as made explicit in [6] to prove the existence (and local uniqueness) of several different steady states of the PFC equation (1). In Figure 1, we provide some examples.

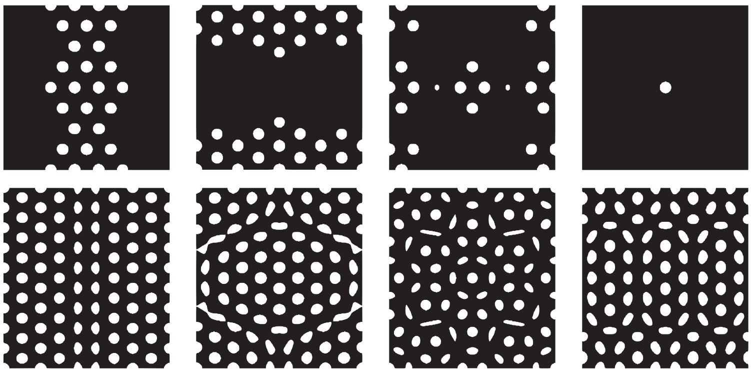

FIGURE 1. Rigorously validated steady states of the PFC equation (1).

One of the open question remaining from this work concerns the existence of connecting orbits. In Figure 2, we consider the parameters $(\bar{\psi}, \beta) = (0.07, 0.025)$, use the very small domain $(N_x, N_y) = (2, 1)$, and we provide a *connection energy diagram*, where arrows represent likely connections (open question).

REFERENCES

[1] K. R. Elder, M. Katakowski, M. Haataja, and M. Grant, *Modeling elasticity in crystal growth*, Physical Review Letters, vol. 88, p. 245701, 2002.

[2] T. V. Ramakrishnan and M. Yussouff, *First-principles order-parameter theory of freezing*, Phys. Rev. B 19, 2775, 1979.

[3] G. Martine La Boissonière, R. Choksi, K. Barmak, and S. Esedoḡlu, *Statistics of grain growth: experiment versus the Phase-Field-Crystal and Mullins models*, Materialia, p. 100280, 2019.

[4] D. Shirokoff, R. Choksi, and J.-C. Nave, *Sufficient conditions for global minimality of metastable states in a class of non-convex functionals: a simple approach via quadratic lower bounds*, Journal of Nonlinear Science, vol. 25, no. 3, pp. 539–582, 2015.

[5] J. B. van den Berg and J. P. Lessard, *Rigorous numerics in dynamics*, Notices of the American Mathematical Society, vol. 62, no. 9, pp. 1057–1061, 2015.

[6] Gabriel Martine-La Boissoniere and Rustum Choksi and Jean-Philippe Lessard, *Microscopic Patterns in the 2D Phase-Field-Crystal Model*, arXiv:2102.02338, 2021.

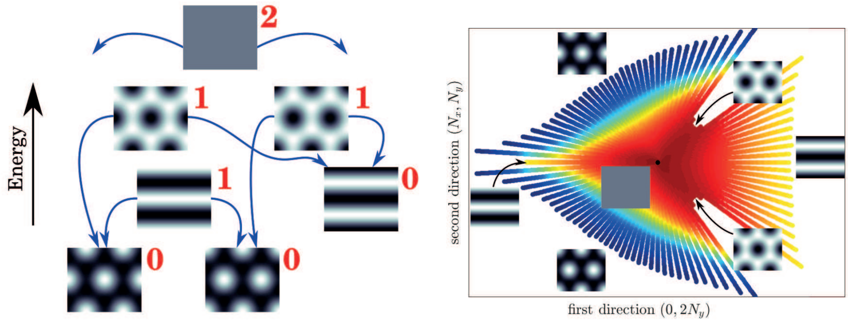

FIGURE 2. Connection diagram (a) where arrows represent likely connections; the constant state is connected to all others. The vertical axis gives the ordering in energy while the numbers give the Morse index. Energy visualization with respect to the unstable directions of the constant state. This diagram illustrates how the unstable directions combine to transform the constant state into other lower energy states. (b) The unstable directions serve as the main axes and the lines represent different initial perturbations. The length of the lines indicate the number of PFC steps before the flows becomes close to the connecting steady states. Colors represent energy (red for high and blue for low energy).

Bifurcation and stability of frequency combs modeled by the Lugiato-Lefever equation

MARIANA HARAGUS

(joint work with Lucie Delcey, Mathew A. Johnson, Wesley R. Perkins, and Björn de Rijk)

We consider the Lugiato-Lefever equation (LLE)

$$\psi_t = -i\beta\psi_{xx} - (1 + i\alpha)\psi + i|\psi|^2\psi + F, \tag{1}$$

where $\psi(x, t)$ is a complex-valued function depending on a temporal variable t and a spatial variable x, the parameters α, β are real, and F is a positive constant. This NLS-type equation with damping, detuning, and driving was derived in nonlinear optics by Lugiato and Lefever [9]. More recently, LLE was obtained as a model for frequency combs (optical signals which consist of a superposition of modes with equally spaced frequencies and are stationary in a suitable reference frame) generated in whispering-gallery-mode resonators [1]. In this context, $\psi(x, t)$ represents the field envelope, α the detuning parameter, F the driving term, and β the dispersion parameter which may be positive (normal dispersion) or negative (anomalous dispersion).

While extensively studied in the physics literature (e.g., see [2] and the references therein), there are relatively few rigorous mathematical studies of this equation. The main mathematical questions concern the existence and the stability of its steady waves, in particular of solitary and periodic waves. We refer to [3, 5, 6, 10, 11] for several existence results, mainly based on tools from bifurcation theory, and to [4, 7, 8, 12] for some recent stability results. Here we focus on periodic waves and the stability results from [3, 4, 7, 8]. We point out that the stability of solitary waves is a largely open question.

Existence of periodic waves. Local bifurcation theory provides efficient tools for the study of the existence of periodic waves. The partial differential equation (1) is treated as an infinite-dimensional dynamical system of the form

$$\frac{dU}{dt} = \mathcal{G}(U, \beta, \alpha, F), \tag{2}$$

in which $U(t)$ represents the real and imaginary parts of $\psi(\cdot, t)$. Taking as phase space for this dynamical system a space consisting of periodic functions, steady periodic waves of (1) become equilibria of (2). Then starting from simple constant solutions, which can be explicitly computed, we study their stability and identify the bifurcation points. The dynamical system being infinite-dimensional, a center manifold reduction is used for the study of local bifurcations. The resulting reduced system is a two-dimensional system of ordinary differential equations which precisely describes the local dynamics close to bifurcation points. We prove that a steady bifurcation with $O(2)$ symmetry occurs which, depending upon the values of the parameters, may be supercritical or subcritical. We construct in this way many different families of steady periodic waves for (1) which bifurcate from constant solutions (see [3, 4] for details).

Stability of periodic waves. Stability properties of periodic waves strongly depend upon the class of perturbations: co-periodic perturbations (periodic perturbations which have the same period as the wave), subharmonic perturbations (periodic perturbations with period equal to an integer multiple N of the period of the wave), or localized perturbations (e.g., integrable on the real line). Notice that instability for co-periodic or subharmonic perturbations implies instability for localized perturbations.

It turns out that the bifurcation analysis mentioned above also allows to determine the stability of the bifurcating periodic waves for co-periodic and subharmonic perturbations. It is shown in [4] that the constructed periodic waves are unstable for subharmonic perturbations with integer multiple N large enough, and consequently also for localized perturbations, except for one family of periodic waves which is stable for all subharmonic perturbations, i.e., for all N. We point out that in these arguments the integer N must be fixed, and that the resulting stability properties do not hold uniformly in N [7].

These stable periodic waves bifurcate supercritically in the case of anomalous dispersion, $\beta < 1$, for any fixed parameter $\alpha < 41/30$ and bifurcation parameter $F^2 = F_1^2 + \mu$, for sufficiently small $\mu > 0$, where $F_1^2 = (1 - \alpha)^2 + 1$, a parameter regime already discussed in the original paper by Lugiato and Lefever [9]. Furthermore, it was shown in [3] that for localized perturbations these periodic waves are diffusively spectrally stable in the sense of the following definition.

Definition. *Consider a smooth T-periodic stationary solution ϕ of* (1) *and denote by $\mathcal{A}[\phi]$ the linear operator given by the linearization of* (1) *at ϕ. The periodic solution ϕ is said to be* diffusively spectrally stable *provided the following conditions hold:*

(1) *the spectrum of the linear operator $\mathcal{A}[\phi]$ acting in $L^2(\mathbb{R})$ satisfies*

$$\sigma_{L^2(\mathbb{R})}(\mathcal{A}[\phi]) \subset \{\lambda \in \mathbb{C} : \Re(\lambda) < 0\} \cup \{0\};$$

(2) *there exists $\theta > 0$ such that for any $\xi \in [-\pi/T, \pi/T)$ the real part of the spectrum of the Bloch operator $\mathcal{A}_\xi[\phi] := e^{-i\xi x}\mathcal{A}[\phi]e^{i\xi x}$ acting in $L^2(0,T)$ satisfies*

$$\Re\left(\sigma_{L^2_{\mathrm{per}}(0,T)}(\mathcal{A}_\xi[\phi])\right) \leq -\theta\xi^2;$$

(3) *$\lambda = 0$ is a simple eigenvalue of $\mathcal{A}_0[\phi]$ with associated eigenvector the derivative ϕ' of the periodic wave.*

Nonlinear modulational stability. Nonlinear stability results for co-periodic and subharmonic perturbations exploit the existence of a spectral gap (the spectrum of the linear operator $\mathcal{A}[\phi]$ lies in the open left half complex plane at a positive distance from the imaginary axis except for an eigenvalue at the origin which is due to the translational invariance of the system). Localized perturbations yield the absence of a spectral gap, hence requiring substantially different methods of analysis (with origins in the pioneering work of Schneider in the nineties).

The study of the decay properties of the linear operator $\mathcal{A}[\phi]$ acting in $L^2(\mathbb{R})$, i.e., linear stability against localized perturbations, is an intermediate step. For the periodic waves of (1) such estimates were obtained in [7], and then the nonlinear stability analysis was carried out in [8]. The following result holds for any diffusively spectrally stable steady periodic solution of (1).

Theorem. *Suppose ϕ is a smooth T-periodic steady solution of* (1) *that is diffusively spectrally stable. Then, there exist constants $\varepsilon, M > 0$ such that, whenever $v_0 \in L^1(\mathbb{R}) \cap H^4(\mathbb{R})$ satisfies*

$$E_0 := \|v_0\|_{L^1 \cap H^4} < \varepsilon,$$

there exist functions $\tilde{v}, \gamma \in C\big([0,\infty), H^4(\mathbb{R})\big) \cap C^1\big([0,\infty), H^2(\mathbb{R})\big)$, with $\tilde{v}(0) = v_0$ and $\gamma(0) = 0$ such that $\psi(t) = \phi + \tilde{v}(t)$ is the unique global solution of (1) *with initial condition $\psi(0) = \phi + v_0$, and the inequalities*

$$\max\{\|\psi(t) - \phi\|_{L^2}, \|\gamma(t)\|_{L^2}\} \leq ME_0(1+t)^{-\frac{1}{4}},$$

and

$$\max\{\|\psi(\cdot - \gamma(\cdot,t),t) - \phi\|_{L^2}, \|\partial_x\gamma(t)\|_{H^3}, \|\partial_t\gamma(t)\|_{H^2}\} \leq ME_0(1+t)^{-\frac{3}{4}},$$

hold for all $t \geq 0$.

We expect that the method used in the proof of this result can be adapted to establish a nonlinear stability result for subharmonic perturbations which is uniform in N, as this was done for linear stability in [7].

References

[1] Y. K. Chembo and C. R. Menyuk, *Spatiotemporal Lugiato-Lefever formalism for Kerr-comb generation in whispering-gallery-mode resonators*, Phys. Rev. A **87** (2013), 053852.

[2] Y. K. Chembo, D. Gomila, M. Tlidi, and C. R. Menyuk, *Topical issue: theory and applications of the Lugiato-Lefever equation*, Eur. Phys. J. D **71**, 2017.

[3] L. Delcey and M. Haragus, *Periodic waves of the Lugiato-Lefever equation at the onset of Turing instability*, Philos. Trans. Roy. Soc. A **376** (2018), 20170188.

[4] L. Delcey and M. Haragus, *Instabilities of periodic waves for the Lugiato-Lefever equation*, Rev. Roumaine Math. Pures Appl. **63** (2018), 377–399.

[5] C. Godey, *A bifurcation analysis for the Lugiato-Lefever equation*, Eur. Phys. J. D **71** (2017), 131.

[6] S. Hakkaev, M. Stanislavova, and A. G. Stefanov, *On the generation of stable Kerr frequency combs in the Lugiato-Lefever model of periodic optical waveguides*, SIAM J. Appl. Math. **79** (2019), 477–505.

[7] M. Haragus, M. A. Johnson, and W. R. Perkins, *Linear modulational and subharmonic dynamics of spectrally stable Lugiato-Lefever periodic waves*, J. Differential Equations **280** (2021), 315–354.

[8] M. Haragus, M. A. Johnson, W. R. Perkins, and B. de Rijk, *Nonlinear modulational of spectrally stable Lugiato-Lefever periodic waves*, submitted.

[9] L. A. Lugiato and R. Lefever, *Spatial dissipative structures in passive optical systems*, Physical Review Letters **58** (1987), 2209.

[10] R. Mandel and W. Reichel, *A priori bounds and global bifurcation results for frequency combs modeled by the Lugiato-Lefever equation*, SIAM J. Appl. Math. **77** (2017), 315–345.

[11] T. Miyaji, I. Ohnishi, and Y. Tsutsumi, *Bifurcation analysis to the Lugiato-Lefever equation in one space dimension*, Phys. D **239** (2010), 2066–2083.

[12] M. Stanislavova and A. G. Stefanov. *Asymptotic stability for spectrally stable Lugiato-Lefever solitons in periodic waveguides*, J. Math. Phys. **59** (2018), 101502.

Some computer-assisted proofs for waves

Maxime Breden

(joint work with Jan Bouwe van den Berg, Claire Chainais-Hillairet, Jean-Philippe Lessard, Maxime Murray, Antoine Zurek)

The last decades have seen the development of computer-assisted proofs for dynamical systems, which allow the quantitative descriptiveness of numerical simulations to be combined with the guarantees of mathematical proofs [3]. These new techniques often perfectly complement the set of already existing mathematical tools that we have at our disposal to study dynamical systems. Indeed, rigorous numerics and computer-assisted proofs are by design well adapted to treat a given – non perturbative and non asymptotic – parameter set, in contrast to many pen and paper techniques (like for instance geometric singular perturbation theory, to name one which was mentioned regularly during this workshop) which do focus on regimes where some parameters are very small (or very large).

There were two other presentations in this workshop, by Jean-Philippe Lessard and Jonathan Jacquette, which made crucial usage of these computer-assisted techniques to study patterns generated by dynamical systems. Here we complement these results by giving two examples of situations where wave-like phenomena can also be rigorously studied with computer assistance.

The first example is the Diffusion Poisson Coupled Model (DPCM), which is a free boundary problem introduced in the context of the underground storage of nuclear wastes [1]. The DPCM aims at predicting the corrosion process which can deteriorate the steel canisters protecting the nuclear wastes, and describes the evolution of an oxide layer. It consists in drift-diffusion equations for the involved charge carriers (ferric cations, electrons and oxygen vacancies), which are coupled via a Poisson equation for the electric potential. Another (highly nonlinear) coupling is present in the Robin boundary conditions, which describe the kinetics of the electro-chemical reactions at the boundaries of the oxide layer. For a complete and precise description of the mathematical model, see e.g. [5] and the references therein.

The mathematical study of the DPCM has proven very challenging, and the few existing results can only handle simplified versions of the model, where some of the couplings are ignored [9]. On the other hand, numerical schemes have been developed to study the full DPCM, and numerical experiments leading to conclusive comparison with real-life data have been conducted [1, 2]. These simulations suggest the apparition of a kind of traveling wave solution, or pseudo-stationary state, where both interfaces of the oxide layer move at a same constant speed, with a fixed profile for the densities of the charge carrier inside the oxide layer. Such solutions were investigated both numerically and theoretically in [8], but again their existence could only be proven for a simplified model.

Using computer-assisted techniques, together with Claire Chainais-Hillairet and Antoine Zurek we were able to prove the existence of such a pseudo-stationary state for the full DPCM, for physically relevant parameter values [5]. Besides, thanks to the constructive nature of these techniques, which give fully explicit and guaranteed a posteriori error estimates between a numerically computed approximate solution and the true solution that is proven to exist, we also obtain a very precise description of the solution, including a tight and certified enclosure of the speed at which the oxide layer progresses, which is of course of the uttermost importance in practice. Another highly relevant issue is that of the stability of the obtained pseudo-stationary state. Numerical simulations suggest that the validated solution is indeed stable, and possibly globally attracting (?), but for the moment these questions remain open.

The second example is concerned with actual traveling waves defined on the whole real line, as opposed to the pseudo-stationary solutions from the DPCM which live on a bounded domain, and for which the computer-assisted proof is more akin to that of a steady state. The model under consideration is the so-called *suspension bridge equation*

$$\partial_{tt} u = -\partial_{xxxx} u - e^u + 1,$$

where $u = u(t, x)$ describes the deflection of the roadway from the rest state $u = 0$ as a function of time t and the spatial variable x representing the direction of traffic.

When this equation was introduced [10], the existence of a traveling wave solution with wave speed c was conjectured for every c^2 in $(0, 2)$. Many partial answers to this conjecture were subsequently obtained, including the existence of a traveling wave solution with wave speed c for *almost all* c^2 in $(0, 2)$ [12] and for every c^2 in $(0, 0.5516)$ [11], both using variational methods, as well as the existence of *at least* 36 traveling wave solutions with wave speed $c = 1.3$ [6], this time using computer-assisted techniques.

Also using computer-assisted techniques, together with Jan Bouwe van den Berg, Jean-Philippe Lessard and Maxime Murray, we proved in [4] the existence of a traveling wave solution with wave speed c for all c^2 in $[0.5, 1.9]$, which amounts to proving the existence of a homoclinic orbit for the dynamical system associated to

$$u'''' + c^2 u'' + e^u - 1 = 0,$$

for all c^2 in $[0.5, 1.9]$. One of the main difficulty in carrying out a computer-assisted proof for such solutions lies in the fact that homoclinic orbits are defined on $\mathbb{R}$, which is unbounded. In order to circumvent this issue, we first make use of the parameterization method [7] to compute and rigorously validate local stable and unstable manifolds at the origin, and then consider a boundary value problem to connect these two manifolds, the corresponding orbit being now defined on a bounded interval. This yields a computer-assisted proof of existence of a traveling wave for a fixed value of c. We then once again use the robustness inherent to these techniques, which is made explicit via a uniform contraction mapping theorem, in order to extend the proof to a whole interval of values of c.

It should be noted that our results could *in principle* be extended to larger closed interval of values of c^2 contained in $(0, 2)$, but definitely not to $(0, 2)$ itself, because the problem becomes singular at both ends of the interval $(0, 2)$, while the techniques from [11] happen to work only for c somewhat close to 0. This illustrates the aforementioned complementary between computer-assisted techniques and more classical pen and paper approaches. The only part of the conjecture that remains open is thus for c^2 close to 2.

References

[1] Bataillon, C., Bouchon, F., Chainais-Hillairet, C., Desgranges, C., Hoarau, E., Martin, F., Perrin, S., Tupin, M., and Talandier, J. Corrosion modelling of iron based alloy in nuclear waste repository. *Electrochimica Acta 55*, 15 (2010), 4451–4467.

[2] Bataillon, C., Bouchon, F., Chainais-Hillairet, C., Fuhrmann, J., Hoarau, E., and Touzani, R. Numerical methods for the simulation of a corrosion model with moving oxide layer. *Journal of Computational Physics 231*, 18 (2012), 6213–6231.

[3] J. B. van den Berg and J.-P. Lessard. Rigorous numerics in dynamics. *Notices Amer. Math. Soc.*, 62(9), 2015.

[4] van den Berg, J. B., Breden, M., Lessard, J.-P., and Murray, M. Continuation of homoclinic orbits in the suspension bridge equation: a computer-assisted proof. *J. Differential Equations 264*, 5 (2018), 3086–3130.

[5] Breden, Maxime, Chainais-Hillairet, Claire, and Zurek, Antoine. Existence of traveling wave solutions for the diffusion poisson coupled model: a computer-assisted proof. *ESAIM: M2AN 55*, 4 (2021), 1669–1697.

[6] Breuer, B., Horák, J., McKenna, P., and Plum, M. A computer-assisted existence and multiplicity proof for travelling waves in a nonlinearly supported beam. *J. Differential Equations 224*, 1 (2006), 60–97.

[7] Cabré, X., Fontich, E., and de la Llave, R. The parameterization method for invariant manifolds. III. Overview and applications. *J. Differential Equations 218*, 2 (2005), 444–515.

[8] Chainais-Hillairet, C., and Gallouët, T. O. Study of a pseudo-stationary state for a corrosion model: Existence and numerical approximation. *Nonlinear Analysis: Real World Applications 31* (2016), 38–56.

[9] Chainais-Hillairet, C., and Lacroix-Violet, I. On the existence of solutions for a drift-diffusion system arising in corrosion modeling. *Discrete & Continuous Dynamical Systems-B 20*, 1 (2015), 77.

[10] Chen, Y., and McKenna, P. Traveling waves in a nonlinearly suspended beam: theoretical results and numerical observations. *Journal of Differential Equations 136*, 2 (1997), 325–355.

[11] Santra, S., and Wei, J. Homoclinic solutions for fourth order traveling wave equations. *SIAM journal on mathematical analysis 41*, 5 (2009), 2038–2056.

[12] Smets, D., and van den Berg, J. B. Homoclinic solutions for swift–hohenberg and suspension bridge type equations. *Journal of Differential Equations 184*, 1 (2002), 78–96.

Quenched stripes: wavenumber selection and dynamics

Ryan Goh

Quenching mechanisms are a potent tool for controlling and mediating pattern-forming phenomena in a variety of physical systems. Broadly, an external mechanism spatially progressively moves across a system, bifurcating or exciting pattern-forming instabilities. By controlling the exact nature of this quenching process, including its geometry and speed of propagation, one can control the pattern formed in the wake. While examples of such a mechanism arise in diverse areas such as chemical precipitation and deposition in the wake of a traveling reaction front [12], water-jet cutting and etching [5], chemical evaporation and de-wetting [17, 15], directional quenching of liquid melts [4, 16], and formation of crystalline latices [2], one physical system which nicely exemplifies a quenching process is the light-sensitive, diffusion limited, CDIMA reaction [13]. Such a system exhibits a Turing instability which is suppressed when exposed to high-intensity light. Turning the light off homogeneously excites unstable modes of all orientations leading to a disorganized arrangement of locally coherent patterns with defects in between. If instead a mask is moved across the domain, progressively blocking the light, a more coherent, and nearly defect-free pattern can be formed [14, 11]. Furthermore, by changing the mask speed and shape, different striped patterns can be selected.

This talk gives an overview of recent works [1, 3, 7, 6, 9, 10, 8, 18] which study pattern selection in the wake of quenching processes. To fix the scene, we discuss results and phenomena in the prototypical two-dimensional Swift-Hohenberg equation

$$u_t = -(1+\Delta)^2 u + \mu u - u^3, \quad u \in \mathbb{R},\ (x,y,t) \in \mathbb{R}^2 \times \mathbb{R}_+, \quad \Delta = \partial_x^2 + \partial_y^2. \tag{1}$$

Here u is an order parameter which originally represented the perturbation from a pure conductive state in Rayleigh-Bénard convection, and μ the bifurcation parameter controlling the onset of convective roll formation. From a phenomenological standpoint, this equation is arguably the simplest scalar equation which forms stable periodic patterns.

A quenching mechanism can be modeled in this setting by replacing μ with a spatio-temporal heterogeneity

$$(2)\quad u_t = -(1+\Delta)^2 u + \rho(x,y,t)u - u^3, \quad \rho(x,y,t) = \begin{cases} \mu, & (x,y) \in \Omega_t, \\ -\mu, & (x,y) \in \Omega_t^c, \end{cases},$$

where $\mu > 0$ and Ω_t is some time-dependent, and evolving domain, so that $u \equiv 0$ is Turing unstable in Ω_t and stable in its complement. The simplest quenching mechanism one could study is a planar, or *directional*, quench where the boundary $\partial\Omega_t$ is a line which rigidly propagates in the normal direction at a fixed speed c. In particular, one could set $\rho(x,y,t) = -\mu \mathrm{sgn}(x - c_x t)$.

To organize dynamics of patterns in the wake of a directional quench, one considers travelling wave type solutions to (2) of the form $u(x,y,t) = v(x - c_x t, k_y(y - c_y t))$, which are 2π-periodic in the second variable and are posed in the horizontal frame moving with the quenching speed c_x. In terms of the new variables $\tilde{x} = x - c_x t$, $\tilde{y} = k_y(y - c_y t)$, one finds v satisfies a pseudo-elliptic equation on which we append asymptotic boundary conditions to look for pattern-forming front solutions

(3)
$$0 = -(1 + \partial_{\tilde{x}}^2 + k_y^2 \partial_{\tilde{y}}^2)^2 v + \rho(\tilde{x})v - v^3 + c_x\left(\partial_{\tilde{x}} + k_y \partial_{\tilde{y}}\right) v, \quad u(\tilde{x}, \tilde{y} + 2\pi) = u(\tilde{x}, \tilde{y})$$

(4)
$$\lim_{\tilde{x} \to -\infty} |v(\tilde{x},\tilde{y}) - u_p(k_x \tilde{x} + \tilde{y}; k)| = 0, \quad \lim_{\tilde{x} \to +\infty} v(\tilde{x},\tilde{y}) = 0.$$

Here $k = \sqrt{k_x^2 + k_y^2}$ gives the bulk wavenuber, k_x and k_y give the horizontal and vertical wavenumber respectively of the asymptotic stripe state $u_p(\theta; k)$, which itself is an equilibria of (1) satisfying the periodic equilibrium equation

$$0 = -(1 + k^2 \partial_\theta^2)^2 u_p + \mu u_p - u_p^3, \qquad u_p(\theta + 2\pi; k) = u_p(\theta; k).$$

Solutions of (3) can be coarsely categorized by the parameter set

$$\mathcal{M} := \{(c_x, k_y, k_x) \,:\, (3) \text{ has a solution}\},$$

with the geometry of this variety giving insight into the bifurcation structure and geometry of the solution space. We highlight the results of numerical continuation, rigorous analysis, as well as formal asymptotic calculations, which describe this set.

This talk discusses how different approaches, from dynamical systems theory, functional analysis, and modulational theory, can be used to study stripe formation in various orientation and growth regimes. We also highlight how these ideas can be applied to other prototypical pattern-forming equations such as the anisotropic Swift-Hohenberg equation, a Swift-Hohenberg equation with subcritical cubic-quintic nonlinearity, the complex Ginzburg-Landau equation, as well a two-component reaction-diffusion model for the CDIMA system mentioned above.

References

[1] Avery, M. and Goh, R. and Goodloe, O. and Milewski, A. and Scheel, A. *Growing stripes, with and without wrinkles.*, SIAM Journal on Applied Dynamical Systems **18**(2) (2019),1078-1117.

[2] Akamatsu, S. and Bottin-Rousseau, S. and Faivre, G. *Experimental Evidence for a Zigzag Bifurcation in Bulk Lamellar Eutectic Growth.*, Phys. Rev. Lett. **93**(17) (2004).

[3] Chen, K. and Deiman, Z. and Goh, R. and Jankovic, S. and Scheel, A. *Strain and defects in oblique stripe growth.*,Multiscale Model. Simul. **19**(3), (2021) 1236–1260.

[4] Foard, E. M. and Wagner, A. J. *Survey of morphologies formed in the wake of an enslaved phase-separation front in two dimensions*, Phys. Rev. E **85**(1) (2012).

[5] Friedrich, R. and Radons, G. and Ditzinger, T. and Henning, A. *Ripple Formation through an Interface Instability from Moving Growth and Erosion Sources.*, Phys. Rev. Lett. **85**(23) (2000), 4884–4887.

[6] Goh, R. "Quenched Stripes: Wavenumber Selection and Dynamics." DSWeb, July 2021, https://dsweb.siam.org/The-Magazine/All-Issues/quenched-stripes-wavenumber-selection-and-dynamics-1.

[7] Goh, R. and de Rijk, B. *Spectral stability of pattern-forming fronts in the complex Ginzburg-Landau equation with a quenching mechanism.* arXiv preprint arXiv:2006.15083 (2020).

[8] Goh, R. and Scheel, A. *Hopf bifurcation from fronts in the Cahn–Hilliard equation.* Arch. Rat. Mech. Anal. **217**(3) (2015), 1219–1263.

[9] Goh, R. and Scheel, A. *Pattern-forming fronts in a Swift-Hohenberg equation with directional quenching – parallel and oblique stripes.* J. Lon. Math. Soc., **98**(1) (2019), 104-128.

[10] Goh, R. and Scheel, A. *Triggered fronts in the complex Ginzburg Landau equation.* J. Nonlinear Sci., **24**(1) (2014), 117–114.

[11] Konow, C. and Somberg, N.H. and Chavez, J. and Epstein, I.R. and Dolnik, M.. *Turing patterns on radially growing domains: experiments and simulation*, Physical Chemistry Chemical Physics **21**(12) (2019), 718–6724.

[12] Thomas, S. and Lagzi, I. and Molnár, F. and Rácz, Z. *Helices in the wake of precipitation fronts.*, Phys. Rev. E **88**(2) (2013).

[13] Lengyel, I. and Epstein, I.R. *A chemical approach to designing Turing patterns in reaction-diffusion systems.*, Proceedings of the National Academy of Sciences **89**(9) (1992), 3977–3979.

[14] Míguez, D. G. and Dolnik, M. and Munuzuri, A. P. and Kramer, L., *Effect of axial growth on Turing pattern formation*, Physical review letters **96**(4) (2006).

[15] Thiele, U. *Patterned deposition at moving contact lines.*, Advances in Colloid and Interface Science **206**(0) (2014), 399 - 413.

[16] Tsukada, T. and Kurita, R. *A topological transition by confinement of a phase separating system with radial quenching*, Scientific reports **9**(1) (2012), 1-10.

[17] Wilczek, M. and Tewes, W. B.H. and Gurevich, S. V. and Köpf, M. H. and Chi, L. F. and Thiele, U. *Modelling Pattern Formation in Dip-Coating Experiments.*, Math. Model. Nat. Phenom. **10**(4) (2015), 44-60.

[18] Scheel, A., Weinburd, Jasper *Wavenumber selection via spatial parameter jump* Philos. Trans. Roy. Soc. A. **376** (2117) (2018).

Pulse replication and slow absolute spectrum in the FitzHugh–Nagumo system

Paul Carter

(joint work with Jens D. M. Rademacher, Björn Sandstede)

We consider the FitzHugh–Nagumo equation in the form

$$\begin{aligned} u_t &= u_{xx} + u(u-a)(1-u) - w \\ w_t &= \varepsilon(u - \gamma w) \end{aligned} \tag{1}$$

where $a < 1/2$, $0 < \varepsilon \ll 1$ and $\gamma > 0$ is taken small enough so that $(u, w) \equiv (0, 0)$ is the only homogeneous equilibrium of (1). The system (1) is a simplified model of nerve impulse propagation, which is known to admit families of traveling pulse solutions, which are localized in space and bi-asymptotic to $(u, w) = (0, 0)$. Such waves are solutions of the slow/fast traveling wave ODE

$$\begin{aligned} u' &= v \\ v' &= cv - u(u-a)(1-u) + w \\ w' &= \frac{\varepsilon}{c}(u - \gamma w) \end{aligned} \tag{2}$$

where $' = \frac{\mathrm{d}}{\mathrm{d}\xi}$ and $\xi = x + ct$ is the traveling wave coordinate with speed c.

In the region $a \approx 0$, near the boundary between excitable and oscillatory dynamics in (1), these traveling pulses can exhibit a variety of replication phenomena. In particular, upon parameter continuation in the parameters (a, c), a single traveling pulse can grow into a double pulse via a series of folds in parameter space along a so-called homoclinic banana [4], in a phenomenon we refer to as parametric pulse replication; see Fig. 1. The secondary pulse grows from the tail of the primary pulse in a manner resembling a canard explosion [2, 3] in the traveling wave ODE (2). This replication event appears to guide the time dynamics in the PDE (1): when taking one of the traveling pulses near the first fold along the transition and using this as initial data for a direct simulation in (1), one observes temporal pulse replication events in which the pulse grows additional pulses in its wake as time evolves; see Fig. 2.

This motivates us to consider the temporal stability of the intermediate traveling pulses along the single-to-double pulse transition which occurs along the homoclinic banana. Numerical spectral computations show that while the single pulse is initially stable, as it passes through each successive fold along the transition, eigenvalues accumulate on the positive real axis until approximately halfway through the transition, after which all such eigenvalues move into the left half plane except for one; see Fig. 1. In [1], we show that this phenomenon is due to a novel mechanism for eigenvalue accumulation in multiple timescale systems, which we call the *slow absolute spectrum*.

In order to understand this accumulation of eigenvalues, we consider the eigenvalue problem obtained by linearizing (1) in a co-moving frame about the traveling pulse. This eigenvalue problem inherits the slow/fast structure of (2). The traveling pulses are built from perturbations of orbits obtained by gluing portions of

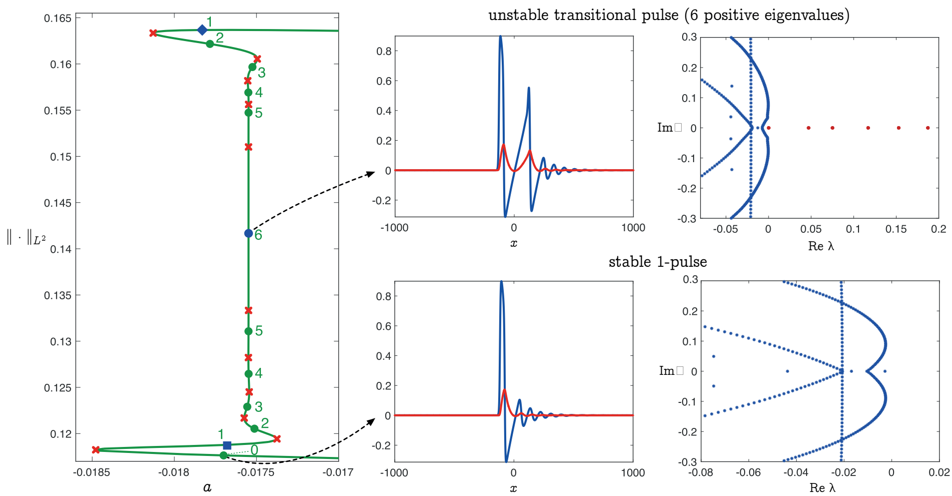

FIGURE 1. (Left) Bifurcation diagram of the 1-to-2-pulse transition obtained by continuing in the parameters (a, c) in (2) for fixed $\varepsilon = 0.01, \gamma = 2$. Red crosses denote fold points, and the number of unstable PDE eigenvalues is given for profiles along the transition marked with a colored bullet/shape. (Right) Sample solution profiles (u blue, w red) and their spectra.

the critical manifold $\mathcal{M} = \{v = 0, w = u(u-a)(1-u)\}$ with fast jumps between the different branches of $\mathcal{M}$ [3]. One finds that pulses along the first part of the transition spend increasing (spatial) times along a portion of $\mathcal{M}$ which exhibits absolute spectrum relative to the asymptotic rest state; that is, when viewed as equilibria, for values of the temporal eigenvalue parameter λ on a interval of the positive real axis, the points along this portion of $\mathcal{M}$ have a different Morse index from that of the asymptotic rest state in any exponentially weighted space. This can lead to an accumulation of eigenvalues, much like that which can arise with pulses which contain a long plateau state, created at T-points [6, 7]. Along the second part of the transition, the length of the trajectory near this portion of the slow manifold decreases, and thus so does the number of accumulating eigenvalues.

We show that this accumulation phenomenon is generic in eigenvalue problems exhibiting an appropriate slow/fast structure, and we validate our hypotheses for (1). The general result is obtained through the use of slowly varying coefficients and exponential trichotomies to obtain a reduced eigenvalue problem on an appropriate center subspace. The eigenvalues are shown to accumulate at a rate $\mathcal{O}(\varepsilon^{-1})$. The above results reported on here have appeared in [1].

This work leaves a number of open directions. We anticipate that the slow absolute spectrum phenomenon can be further generalized and linked to interesting dynamics in related settings. Additionally, the link between the temporal pulse replication in (1) and the eigenvalue accumulation associated with the homoclinic

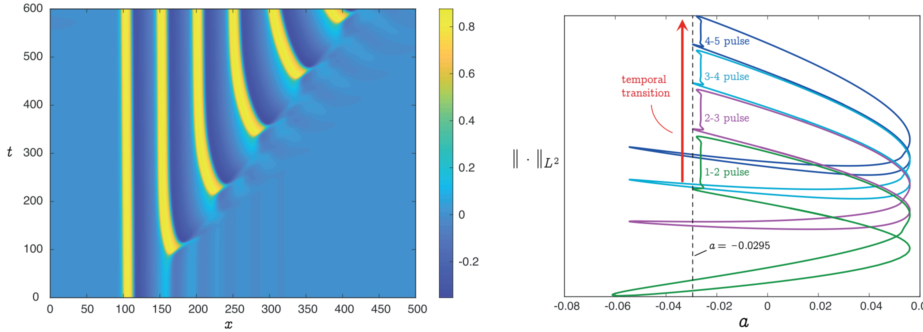

Figure 2. (Left) Spacetime plot of u-profile in (1) exhibiting temporal pulse adding for fixed $a = -0.0295, \varepsilon = 0.015$. (Right) Shown are homoclinic bananas obtained by numerical continuation in (a, c) for fixed $\varepsilon = 0.015, \gamma = 2$. The upper left corner of each banana contains a parametric transition from a spectrally stable n-pulse to an unstable $(n + 1)$-pulse.

banana(s) which describe the parametric pulse replication between traveling n-to-$(n + 1)$ pulses (see Fig 2) has not been established. We are currently exploring this by attempting to obtain a description of the possible reduced dynamics on an invariant manifold describing the temporal pulse adding transitions. Furthermore, simulations suggest that a variety of other replication phenomena are present in the traveling wave ODE, such as homoclinic bananas which connect m and n pulses for different values of m, n, as well as pulse-adding behavior generated by successive canard explosions of periodic wave trains in (2). These phenomena exhibit fold-alignment behavior associated with pulse adding/splitting in other systems [5]; also see Fig 2. These topics are the subject of ongoing and future work.

References

[1] P. Carter, J. D. M. Rademacher and B. Sandstede, *Pulse replication and accumulation of eigenvalues*, SIAM J. Math. Anal. **53** (2021), 3520–3576.

[2] P. Carter and B. Sandstede, *Fast pulses with oscillatory tails in the FitzHugh–Nagumo system*, SIAM J. Math. Anal. **47** (2015), 3393–3441.

[3] P. Carter and B. Sandstede, *Unpeeling a homoclinic banana in the FitzHugh–Nagumo system*, SIAM J. Appl. Dyn. Syst. **17** (2018), 236–349.

[4] A. R. Champneys, V. Kirk, E. Knobloch, B. E. Oldeman, and J. Sneyd, *When Shil'nikov meets Hopf in excitable systems*, SIAM J. Appl. Dyn. Syst. **6** (2007), 663–693.

[5] Y. Nishiura and D. Ueyama, *A skeleton structure of self-replicating dynamics*, Phys. D **130** (1999), 73–104.

[6] B. Sandstede and A. Scheel, *Absolute and convective instabilities of waves on unbounded and large bounded domains*, Phys. D **145** (2000), 233–277.

[7] B. Sandstede and A. Scheel, *Gluing unstable fronts and backs together can produce stable pulses*, Nonlinearity **13** (2000), 1465–1482.

Many-spike limit for pattern formation

Theodore Kolokolnikov

In the first part of the talk, we consider a highly symmetric configuration of N spikes whose locations are located at the vertices of a regular N-gon inside either a unit disk or an annulus. We call such configuration a ring of spikes. For the Schnakenberg model, the ring radius is characterized in terms of the modified Green's function. For a disk, we find that a ring of 9 or more spikes is always unstable with respect to small eigenvalues. Conversely, a ring of 8 or less spikes is stable inside a disk provided that the feed-rate A is sufficiently large. More generally, for sufficiently high feed-rate, a ring of N spikes can be stabilized provided that the annulus is thin enough. As A is decreased, we show that the ring is destabilized due to small eigenvalues first, and then due to large eigenvalues, although both of the thresholds are separated by an asymptotically small amount. For a ring of 8 spikes inside a disk, the instability appears to be supercritical, and deforms the ring into a square-like configuration. For less than 8 spikes, this instability is subcritical and results in spike death.

In the second part of the talk, we study the Gierer-Meinhardt model with heterogeneous precursor gradient in 1 and 2 dimensions. We derive the effective spike density in the limit spikes. This density is shown to be a solution of a separable ODE. In 2D, it involves infinite lattice sums over hexagonal lattices.

References

[1] Theodore Kolokolnikov and Michael Ward, *A ring of spikes*, preprint.
[2] Theodore Kolokolnikov and Juncheng Wei, *Hexagonal spike clusters for some PDE's in 2D*, DCDS-B, 2020(10): 4057-4070.
[3] Theodore Kolokolnikov and Shuangquan Xie, *Spike density distribution for the Gierer-Meinhardt model with precursor*, Physica D, 2019.
[4] Theodore Kolokolnikov and Juncheng Wei, *Pattern formation in a reaction-diffusion system with space-dependent feed-rate*, SIAM Review, 2018.

Spatially localized time-periodic solutions of semilinear wave equations

Wolfgang Reichel
(joint work with Andreas Hirsch, Simon Kohler)

We consider the semilinear wave equation

$$V(x)u_{tt} - \Delta u = \Gamma(x)|u|^{p-1}u \text{ in } \mathbb{R}^N \times \mathbb{R} \tag{1}$$

and we aim at proving the existence of spatially localized, time-periodic solutions (breathers) – which rarely occur in semilinear wave equations. Due to non-constant coefficients the linear wave operator has a space-dependent finite speed of propagation. We consider cases where V is strictly positive or where it may change sign. The latter typically arises when considering travelling waves with speed c of a semilinear wave equation in $\mathbb{R}^{N+1} \times \mathbb{R}$ since then $V(x) = W(x) - c^{-2}$.

We are particularly motivated by an example from [1] where the special case of

$$V(x)u_{tt} - u_{xx} + q(x)u = \pm u^3 \text{ in } \mathbb{R}\times\mathbb{R}$$

is considered with $q(x) = (q_0 - \epsilon^2)V(x)$, a very specific 1-periodic function $V(x)$, and a very specific value of q_0. For small $\epsilon > 0$ the existence of small breathers of size ϵ is proven. The result was obtained by spatial dynamics and center-manifold reduction.

In our approach [3, 4] we use a variational method to establish the existence of breathers for a variety of examples. Finding the temporal period $T = \frac{2\pi}{\omega}$ is part of the problem. Starting with the decomposition

$$u(x,t) = (S\hat{u})(x,t) := \sum_{k\in\mathbb{Z}_{odd}} u_k(x)e^{ik\omega t}, \quad \overline{u}_k = u_{-k}$$

with $\hat{u} = (u_k)_{k\in\mathbb{Z}_{odd}}$, the wave operator $L = V(x)\partial_t^2 - \Delta$ accordingly splits into a family of Schrödinger operators $(L_k)_{k\in\mathbb{Z}_{odd}}$, $L_k = -\Delta - k^2\omega^2 V(x)$ with spectrum $\sigma(L_k)$. Our key assumption (which will be verified in the examples) is that

$$\operatorname{dist}(0,\sigma(L_k)) = O(|k|^\gamma) \text{ as } |k|\to\infty$$

for some $\gamma > 0$, i.e., 0 lies in a spectral gap of L_k which grows in size as k increases. The key assumption can only be verified when $k \neq 0$ and when $V \not\equiv \text{const}$. In order to overcome the first difficulty ($k \neq 0$) we restrict to $T/2$-antiperiodic functions (i.e., $k \in \mathbb{Z}_{odd}$).

We find breathers variationally as critical points of an energy functional. Using the bilinear form b_{L_k} of the operator L_k and the abbreviation $D = \mathbb{R}^N \times (0,T)$ the energy functional takes the form

$$\begin{aligned} J(u) &= \int_D |\nabla u|^2 - V(x)u_t^2 \, d(x,t) - \frac{2}{p+1}\int_D \Gamma(x)|u|^{p+1}\, d(x,t) \\ &= \sum_{k\in\mathbb{Z}_{odd}} b_{L_k}(u_k,u_k) - \frac{2}{p+1}\int_D \Gamma(x)|u|^{p+1}\, d(x,t) \\ &= \|\hat{u}^+\|^2 - \|\hat{u}^-\|^2 - \frac{2}{p+1}\int_D \Gamma(x)|S\hat{u}|^{p+1}\, d(x,t). \end{aligned}$$

Here we have used the fact that the spectral projections of L_k onto the positive and negative spectral subspaces of $\operatorname{dom}(b_k) = H^1(\mathbb{R}^N)$ give rise to the splitting $\operatorname{dom}(b_k) = H^1(\mathbb{R}^N) = H_k^+ \oplus H_k^-$. Using functional calculus to define $|L_k|$ and its bilinear form $b_{|L_k|}$ this allows us to describe the domain of J as all functions $S\hat{u}$ with $\hat{u}$ in

$$\mathcal{H} = \Big\{\hat{u} : \|\hat{u}\|^2 := \sum_{k\in\mathbb{Z}_{odd}} b_{|L_k|}(u_k,u_k) < \infty, \overline{u}_k = u_{-k}\Big\}.$$

The splitting $\operatorname{dom}(b_k) = H^1(\mathbb{R}^N) = H_k^+ \oplus H_k^-$ extends to $\mathcal{H} = \mathcal{H}^+ \oplus \mathcal{H}^-$ with corresponding notation $\hat{u}^\pm \in \mathcal{H}^\pm$. The splitting of the domain of J also suggests how to obtain breathers as critical points (saddle points) of J. The critical level is described as

$$c = \inf_{\substack{\hat{u}^+\in\mathcal{H}^+\\ \|\hat{u}^+\|=1}} \sup_{\substack{t>0\\ \hat{u}^-\in\mathcal{H}^-}} J(t\hat{u}^+ + \hat{u}^-).$$

At this point at least three issues arise which need to be tackled:

(A) When is the key assumption $\mathrm{dist}(0,\sigma(L_k)) = O(|k|^\gamma)$ fulfilled and for which $\gamma > 0$?

(B) For which p^* is there a continuous, locally compact embedding $S : \mathcal{H} \to L^{p+1}(D)$ for all $1 \le p < p^*$?

(C) Is c attained?

Without going into details of how (A)-(C) can be achieved we give a short account of our results.

V, Γ are 2π-periodic in x, cf. [3]**.** Breathers exist in the following cases:

(1) $V(x) = \alpha + \beta\delta^{2\pi}_{per}(x)$, $\beta > 32\alpha > 0$, $\omega = \frac{1}{4\sqrt{\alpha}}$, $\gamma = 2$, $p^* = \infty$

(2) $V(x) = 2\pi$-periodic step function, i.e., 2π-periodic extension of the step function $\alpha 1_{[0,2\theta\pi]} + \beta 1_{[2\theta\pi,2\pi]}$, $\frac{\alpha}{\beta} = \frac{(1-\theta)^2}{\theta^2}$, $0 < \theta \ll \frac{1}{2}$, $\omega = \frac{1}{4\theta\sqrt{\alpha}}$, $\gamma = 1$, $p^* = 3$,

(3) According to [2] there exist $V \in H^r_{per}(\mathbb{R})$ near $V_0 \equiv 1$ for each $r \in [1, \frac{3}{2})$ fulfilling the key assumption with $\gamma = (\frac{3}{2} - r)_-$ and $p^* = \frac{7-2r}{1+2r}$. Furthermore $\omega = \pi(\int_0^{2\pi} \sqrt{V(x)}\,dx)^{-1}$.

V is wave-guide like, cf. [4]**.** Using the idea that u is the profile of a travelling wave $U(x, x_{N+1}, t) = u(x, t - c^{-1}x_{N+1})$ we say that V is wave-guide like if $V(x) = W(x) - c^{-2}$ where $W(x)$ represents the profile of a cylindrical wave-guide with N-dimensional cross-section

$$W(x) = \begin{cases} W_0, & |x| < R, \\ W_1, & |x| > R \end{cases}$$

and $0 < W_1 < c^{-2} < W_0$. Here W_0 stands for the high refractive index inside the wave-guide and W_1 for the low refractive index outside the wave-guide. In fact, this is exactly the condition that allows a guided wave propagating periodically in the x_{N+1} direction with speed c for the linear wave equation $W(x)u_{tt} - \Delta_{N+1}u = 0$. For our nonlinear equation (1) we get that for $\omega = \frac{\pi}{2R}(W_0 - c^{-2})^{-1/2}$ breathers exist in the following cases:

(4) $n = 1$, $\forall$ compact $K \subset \mathbb{R}$: $\inf_K \Gamma > 0$, $\Gamma(x) \to 0$ as $|x| \to \infty$ and $p^* = 3$.

(5) $n = 1$, $\Gamma(x) = \text{const.} > 0$, $R \gg 1$, $p^* = 3$.

(6) $n = 2$, $\Gamma > 0$ is radial function and $p^* = 2$.

N.B.: case (5) is done with a different variational method (dual variational method).

Using the above methodology breathers can be shown to exist also in the following two cases:

(7) For $n = 1$ on a bounded spatial domain $[0, L]$ with zero Dirichlet boundary conditions at 0 and L, $V(x) \equiv 1$, $\omega = \frac{\pi}{2}$, $p^* = \infty$.

(8) If the underlying structure is not the real line but a periodic necklace-graph with $V(x) \equiv 1$, $\omega = \frac{\pi}{2}$, $p^* = \infty$. For the description of the periodic necklace graph and some related results cf. [5].

N.B.: For dimension $n = 1$ we are convinced that in all of the above cases $p^* = \infty$ is the right result for the embedding $S : \mathcal{H} \to L^{p+1}(D)$, $1 \le p < p^*$. We are currently elaborating details.

References

[1] C. Blank, M. Chirilus-Bruckner, V. Lescarret, G. Schneider, *Breather solutions in periodic media*, Comm. Math. Phys. **302** (2011), 815-841.

[2] M. Chirilus-Bruckner, C.E. Wayne, *Inverse spectral theory for uniformly open gaps in a weighted Sturm-Liouville problem*, J. Math. Anal. Appl. **427** (2015), 1168–1189.

[3] A. Hirsch, W. Reichel, *Real-valued, time-periodic localized weak solutions for a semilinear wave equation with periodic potentials*, Nonlinearity **32** (2019), 1408–1439.

[4] S. Kohler, *Variational techniques for breathers in nonlinear wave equations*, Doctoral thesis, Karlsruhe Institute of Technology, to appear (2021).

[5] D. Maier, *Construction of breather solutions for nonlinear Klein-Gordon equations on periodic metric graphs*, J. Differential Equations **268** (2020), 2491–1509.

Origin of Jumping Oscillons in an Excitable Reaction-Diffusion System

Hannes Uecker

(joint work with Edgar Knobloch, Arik Yochelis)

Jumping Oscillons (JOs) are spatially localized relative periodic orbits with strong temporal oscillations that in the lab frame let them disappear and reappear at shifted spatial locations. Such JOs have been identified by direct numerical simulations (DNS) in the excitable regime of certain 3-component reaction diffusion systems of FHN type [YZE06]. In [KUY21] we give a systematic description of branches of traveling wavetrains (TWs), traveling pulses (TPs), and time modulated TPs (mTPs) via numerical continuation and bifurcation, using `pde2path` [Uec21a]. The JOs are found by continuation of mTPs over long branch segments. Additionally, the systems supports various (stable) bound states of JOs and TPs.

References

[KUY21] E. Knobloch, A. Yochelis, H. Uecker. Origin of Jumping Oscillons in an Excitable Reaction-Diffusion System. *Preprint*, 2021.

[Uec21a] H. Uecker. *Numerical continuation and bifurcation in Nonlinear PDEs*. SIAM, Philadelphia, PA, 2021.

[YZE06] L. Yang, A. M. Zhabotinsky, and I. R. Epstein. Jumping solitary waves in an autonomous RD system with subcritical wave instability. *PCCP*, 8:4647–4651, 2006.

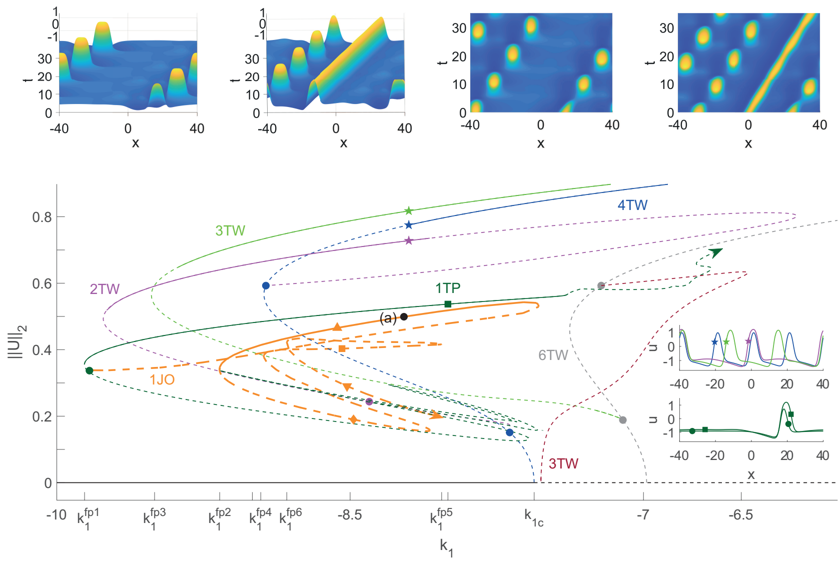

FIGURE 1. Top: samples of 1JO, and of 1P1JO–, 2JO–, and 1P2JO–bound states. Bottom: basic bifurcation diagram of TWs, TPs (see insets for samples), and 1JOs.

Small amplitude approximate localised cellular patches

DAVID J.B. LLOYD
(joint work with Daniel J. Hill, Jason Bramburger)

Localised patches of cellular pattern (see Figure 1) have been known to exist in pattern forming PDE systems for over 20 years where they are numerically found to emerge from a quiescent background state near a Turing/pattern-forming instability [5, 9, 10]. However, there is still no mathematical theory for the emergence of these localised patterns since the spatial dynamics approach [2] does not apply in this setting due to there being no single unbounded direction. Furthermore, at a Turing instability of systems posed in dimensions greater than 1, there is a continua of unstable modes that bifurcate rather than a finite number allowing the tools of centre-manifold reduction to apply. Formally, one could carry out a weakly nonlinear, slowly varying amplitude analysis [4] by supposing the cellular patterns have a certain symmetry but this leads to a system of PDEs that are still difficult to show if there is a fully localised pulse solution [1].

In this talk, we take the simplest pattern-forming system, the Swift-Hohenberg equation [12]

$$(1) \qquad \widehat{u}_t = -\left(1+\Delta\right)^2 \widehat{u} - \mu \widehat{u} + \gamma \widehat{u}^2 - \widehat{u}^3, \qquad (r,\theta) \in \mathbb{R}^+ \times [0, 2\pi),$$

where $\widehat{u} = \widehat{u}(r,\theta,t)$, $\Delta := \left(\partial_{rr} + \frac{1}{r}\partial_r + \frac{1}{r^2}\partial_{\theta\theta}\right)$, $0 < \mu \ll 1$ acts as the bifurcation parameter, and $\gamma \in \mathbb{R}$ is a fixed parameter of the system. The Swift-Hohenberg

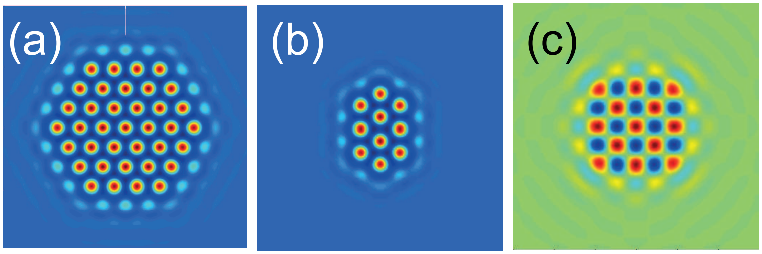

Figure 1. A variety of localised patterns known to exist the Swift-Hohenberg equation (1) (a) localised cellular hexagon patch (b) a localised hexagonal cellular patch but with rhombic super structure and (c) a localised cellular square patch.

equation serves as a prototypical pattern forming system and for purely axisymmetric patterns it has been shown to be a normal form near a Turing instability in general reaction-diffusion systems [11]. We investigate stationary patterns and carry out a finite Fourier decomposition in the angular variable θ of the form

$$\widehat{u}(r,\theta) = u_0(r) + 2\sum_{n=1}^{N} u_n(r)\cos\left(2mn\theta\right), \tag{2}$$

where $N \in \mathbb{N}$ is the truncation order. This decomposition allows us to capture 'approximate' even dihedral lattice patterns, $\mathbb{D}_{2m}$, that are invariant under rotations of $\frac{\pi}{m}$ about its centre; i.e., $\widehat{u}\left(r,\theta\right) = \widehat{u}\left(r,\theta + \frac{\pi}{m}\right)$. Projecting the Swift-Hohenberg equation onto each of the Fourier modes we end up with a a finite Galerkin system

$$0 = L_n(r)u_n + F_n\left(\widehat{u};\mu\right), \qquad \forall n \in [0,N], \tag{3}$$

where $0 < \mu \ll 1$ is the bifurcation parameter, $L_n(r)$ is a non-autonomous linear differential operator depending on the radial variable r, and F_n is the nonlinearity of the system.

One can now study (3) using radial centre-manifold theory/analysis to construct small amplitude bifurcating solutions from $u_n = 0$ at $\mu = 0$ [6, 7, 8, 11]. The main advantage of this approach is that one can now use spatial dynamics to show the existence of a bifurcating small amplitude localised solution to (3) for any m. The approach is applicable to more general systems where one can carry out centre-manifold reduction.

In [3], we discuss the proofs of the following theorems. In order to state our first theorem for the existence of a small amplitude localised solution in (3), we need to make the following hypothesis.

Hypothesis 1. *Fix $m, N \in \mathbb{N}$, and define the vector function $\widetilde{\mathbf{Q}} : \mathbb{R}^{N+1} \to \mathbb{R}^{N+1}$, such that*

$$\left[\widetilde{\mathbf{Q}}(\mathbf{a})\right]_n := 2\sum_{j=1}^{N-n}\cos\left(\frac{2m\pi(n-j)}{3}\right)a_j a_{n+j} + \sum_{j=0}^{n}\cos\left(\frac{2m\pi(n+j)}{3}\right)a_j a_{n-j},$$

for all $n \in [0, N]$*, where* $\left[\widetilde{\mathbf{Q}}(\mathbf{a})\right]_n$ *denotes the* n*'th element of* $\widetilde{\mathbf{Q}}(\mathbf{a})$*. Then, there exists a fixed point* $\mathbf{a}^* \in \mathbb{R}^{N+1}$ *of* $\widetilde{\mathbf{Q}}(\mathbf{a})$*, where* $[\mathbf{a}^*]_n \neq 0$ *for all* $n \in [0, N]$*, such that the linearisation of* $\widetilde{\mathbf{Q}} - \mathbf{I}$ *about* $\mathbf{a}^*$ *is invertible.*

Theorem 1. *Fix* $m, N \in \mathbb{N}$*,* $\gamma \neq 0$*, and assume Hypothesis 1 is met. Then, there is some* $\mu^* > 0$ *such that the truncated Galerkin system* (3) *has a stationary localised* N*-patch solution*

$$u_n(r) = \mu^{\frac{1}{2}} a_n \, (-1)^{mn} \, \frac{\sqrt{3}}{\gamma} \, J_{2mn}(r) + \mathrm{O}(\mu),$$

for each $\mu \in (0, \mu^*)$*, uniformly on bounded intervals* $r \in [0, r_0]$ *as* $\mu \to 0$*, where the coefficients* $\{a_n\}_{n=0}^N$ *satisfy the matching problem* $\widetilde{Q}(\mathbf{a}) = \mathbf{a}$ *where* $\mathbf{a} = [a_0, \ldots, a_N]^T$*.*

For small $N = 1, 2, 3$ and $N = 4$ for the case m is a multiple of 3, we can prove that Hypothesis 1 is met. These small N cases provide excellent initial conditions for numerical continuation algorithms and we are able to find a plethora of different types of localised patterns for arbitrary lattices. In the case of $m = 3$ i.e. hexagonal, $\mathbb{D}_6$, lattice patterns, we have the following theorem for sufficiently large Fourier truncations.

Theorem 2. *There exists an* $N_0 \geq 1$ *such that for all* $N \geq N_0$ *there exists a solution to the fixed point problem in Hypothesis 1, written* $\tilde{a} \in \mathbb{R}^N$*, such that* $\|\tilde{a} - \hat{a}\| \to 0$ *and* $N \to \infty$*, with* $\hat{a} = [\bar{a}(0), \bar{a}(1/N)), \ldots, \bar{a}((N-1)/N)] \in \mathbb{R}^N$ *and* $\bar{a}(t) \in C[0, 1]$ *satisfies*

$$a(t) = 2\int_0^{1-t} a(s)a(t+s)\mathrm{d}s + \int_0^t a(s)a(t-s)\mathrm{d}s, \qquad t \in [0, 1]. \tag{4}$$

This theorem is proved using a combination of a computer-assisted proof for the existence of a $C[0, 1]$ solution to (4) and then using a Newton-Kantovich theorem to prove the existence of a discrete solution near to the continuous one.

While this theorem states that the localised solution we find in Theorem 1 goes to zero as $N \to \infty$, for any finite Fourier truncation one can find a localised $\mathbb{D}_6$ lattice pattern numerically. Furthermore, we find numerically that these localised solutions persist as $N \to \infty$ provided $\mu > 0$. It remains to see if a computer-assisted proof can prove the existence of a localised hexagonal cellular patch in the Swift-Hohenberg equation.

References

[1] A. Doelman, B Sandstede, A. Scheel, G. Schneider, G., *Propagation of hexagonal patterns near onset*, European J. Appl. Math., **14**(1), 85–110, (2003).

[2] M. Haragus, Mariana and G. Iooss, *Local bifurcations, center manifolds, and normal forms in infinite-dimensional dynamical systems*, Springer-Verlag London, Ltd., London; EDP Sciences, Les Ulis, (2011).

[3] D. J. Hill, J. Bramburger, D. J. B. Lloyd, *The existence of small amplitude approximate localised dihedral patterns in the planar Swift-Hohenberg equation*, In preparation, (2021).

[4] R. B. Hoyle, *Pattern Formation*, Cambridge University Press, (2006)

[5] D. J. B. Lloyd, B. Sandstede, D. Avitabile, and A. R. Champneys, *Localized hexagon patterns of the planar Swift–Hohenberg equation*, SIAM Journal on Applied Dynamical Systems, **7**, 1049–1100, (2008).

[6] D. J. B. Lloyd, and B. Sandstede, *Localized radial solutions in the Swift–Hohenberg equation*, Nonlinearity, **22**(2), 485–524, (2009).

[7] McCalla, S., Sandstede, B.: *Spots in the Swift–Hohenberg equation.* SIAM J. Appl. Dyn. Syst. **12**(2), 831–877 (2013).

[8] McQuighan, K., Sandstede, B.: *Oscillons in the planar Ginzburg?Landau equation with 2 : 1 forcing.* Nonlinearity **27**(12), 3073–3116 (2014).

[9] H. Sakaguchi, H. R. Brand, *Stable localized solutions of arbitrary length for the quintic Swift-Hohenberg equation*, Physica D, **97**, 274–285, (1996).

[10] H. Sakaguchi, H. R. Brand, *Stable localized squares in pattern-forming nonequilibrium systems*, Europhysics Letters, **38**, 341, (1997).

[11] A. Scheel, *Radially symmetric patterns of reaction-diffusion systems*, Memoirs of the American Mathematical Society, **165**, 786, (2003).

[12] J. Swift and P. C. Hohenberg, Hydrodynamic fluctuations at the convective instability, Phys. Rev. A **15**(1), 319–328, (1977).

The speed of a random front for stochastic reaction-diffusion equations with strong noise

Carl Mueller

(joint work with Leonid Mytnik, Lenya Ryzhik)

The KPP equation is one of the most widely studied PDE which exhibits a solution $(u(t,x))_{t\geq 0, x\in\mathbf{R}}$ converging to a traveling wave:

$$
\begin{aligned}
\partial_t u &= \partial_x^2 u + u(1-u) \\
u(0,x) &= \mathbf{1}_{(-\infty,0]}(x).
\end{aligned}
\tag{1}
$$

To be precise, there exists a function $C(t)$ and a function $h(x)$ such that $h(x) \to 1$ as $x \to -\infty$ and $h(x) \to 0$ as $x \to +\infty$, such that as $t \to \infty$, $u(t, x - C(t))$ converges uniformly to $h(x)$. Furthermore,

$$
\lim_{t\to\infty} \frac{C(t)}{t} = 2.
$$

These results have been generalized in many directions, see [9, 10].

Our goal is to study the asymptotic traveling wave speed in the presence of random noise. A common motivation for (1) involves the spread of an advantageous gene through the population. Here $u \in [0,1]$ represents the fraction of the local population which has the advantageous gene, and $u(1-u)$ is a competition term proportional to the number of interactions between individuals of the two types. A natural requirement for the noise is that its variance should also be proportional to $u(1-u)$. This leads us to the following equation, in which $\dot{W}(t,x)$ is two-parameter white noise and $\sigma > 0$ is a constant.

$$
\begin{aligned}
\partial_t u &= \partial_x^2 u + u(1-u) + \sigma\sqrt{u(1-u)}\dot{W} \\
u(0,x) &= \mathbf{1}_{(-\infty,0]}(x).
\end{aligned}
\tag{2}
$$

In fact, with probability one for all $t \geq 0$, the wavefront has a (random) right edge defined as

$$R(t) = \sup\{x \in \mathbf{R} : u(t,x) > 0\}$$

(see [7], in which the additive term $u(1-u)$ was replaced by a more general function $f(u)$ satisfying certain conditions. For simplicity, will will only discuss $f(u) = u(1-u)$ here. The noise coefficient was also allowed to be more general.) [7] gave the following asymptotic expansion for $R(t)$ as $t \to \infty$, for small values of σ:

$$\frac{R(t)}{t} = 2 - \pi^2 |\log \sigma^2|^{-2} + O((\log|\log \sigma|)|\log \sigma|^{-3})$$

confirming conjectures in [1, 2, 3].

For small values of σ, solutions to the KPP equation with noise can be thought of as perturbations of solutions to the same equation without noise. But this intuition fails for large σ. Nevertheless, it was proved in [4] that for all $\sigma \geq 0$ there exists a nonrandom speed $V(\sigma)$ such that almost surely

$$\lim_{t\to\infty} \frac{R(t)}{t} = V(\sigma)$$

$$\lim_{\sigma\to\infty} \sigma^2 V(\sigma) \geq 2.$$

Our main result, published in [6], is to prove equality, namely

$$\lim_{\sigma\to\infty} \sigma^2 V(\sigma) = 2.$$

The main ingredients in our proof are:

(A) Scaling, where we write $v(t,x) = u(2\sigma^{-4}t, 2\sigma^{-2}x)$ and verify that v satisfies

$$\partial_t v = \frac{1}{2}\partial_x^2 v + 2\sigma^{-4} v(1-v) + \sqrt{v(1-v)}\dot{W}$$

for a different white noise $\dot{W}(t,x)$.

(B) Using a Girsanov change of measure to reduce the equation to

$$\partial_t v = \frac{1}{2}\partial_x^2 v + \sqrt{v(1-v)}\dot{W}$$

(C) Using results in [8], which state that the wavefront for solutions to the equation from part (B) moves like a Brownian motion.

(D) Splitting up time into stages roughly of length σ^8, and starting the nth stage over again with an initial function $\mathbf{1}_{(-\infty, n\sigma^4]}$. This new initial condition is related to the true solution v by a comparison principle from [5].

References

[1] E. Brunet and B. Derrida, *Shift in the velocity of a front due to a cutoff*, Phys. Rev. E (3), Part A **56** (1997), no. 2, 2597–2604.

[2] E. Brunet and B. Derrida, *Effect of microscopic noise on front propagation*, J. Stat. Phys. **103** (2001), no. 1-2, 269–282.

[3] E. Brunet, B. Derrida, A.H. Mueller, and S. Munier, *Aphenomenologicaltheorygivingthe full statistics of the position of fluctuating pulled fronts*, Phys. Rev. E **73** (2006), 056126, 699–732.

[4] J. Conlon and C. Doering, *On travelling waves for the stochastic Fisher-Kolmogorov-Petrovsky-Piscunov equation*, J. Stat. Phys. **120** (2005), no. 3-4, 421–477.
[5] C. Mueller, *On the support of solutions to the heat equation with noise*, Stochastics Stochastics Rep. **37** (1991), no. 4, 225–245.
[6] Carl Mueller, Leonid Mytnik, and Lenya Ryzhik, *The speed of a random front for stochastic reaction-diffusion equations with strong noise*, Comm. Math. Phys. **384** (2011), no. 2, 699–732.
[7] Carl Mueller, Leonid Mytnik, and Jeremy Quastel, *Effect of noise on front propagation in reaction-diffusion equations of KPP type*, Invent. Math. **184** (2011), no. 2, 405–453.
[8] C. Mueller, R. Tribe, *Finite width for a random stationary interface*, Electron. J. Probab. **2** (1997), no. 7, 27pp.
[9] J. Nolen, J.-M. Roquejoffre, and L. Ryzhik, *Refined long time asymptotics for Fisher-KPP fronts*, Commun. Contemp. Math. **21** (2019), no. 7, 25pp.
[10] M. Roberts, *A simple path to asymptotics for the frontier of a branching Brownian motion*, Ann. Probab. **41** (2013), 3518–3541.

Traveling Fronts in a Model for Social Outbursts

Anna Ghazaryan
(joint work with Marzieh Bakhshi, Vahagn Manukian, Nancy Rodríguez)

Social outbursts like civil unrest, protests, and rioting are expressions of objection towards an idea or action of a government. They often mark dramatic changes in the course of history. The suitable background for outbursts is the social tension. Motivated by the data from the 2005 French riots, Berestycki et al, in [2], introduce a reaction-diffusion model for the dynamics of social unrest u and tension v as functions of the time $\tau > 0$ and space $x \in \mathbb{R}^n$,

$$\left\{ \begin{array}{lcl} u_\tau & = & d_1 \Delta u + r(v) G(u) - \omega u, \\ v_\tau & = & d_2 \Delta v + 1 - h(u) v. \end{array} \right. \tag{1}$$

The model assumes a nearest neighbor contagion and thus there are the diffusion terms for u and v with the respective diffusion coefficients, d_1, $d_2 > 0$. It is assumed that in the absence of v the rioting behavior would decrease proportionally to itself, therefore, $\omega > 0$.

The model takes into account a bandwagon effect (self-excitement) on the level of unrest that turns on when the social tension is high enough. It is modeled by a KPP-type function [3] $G = u(1 - u)$. The bandwagon effect is assumed to be negligible until the social tension v is sufficiently large. The switch mechanism is modeled by the function

$$r(v) = \frac{\Gamma}{1 + e^{-\beta(v-\alpha)}} \quad \text{and} \quad h(u) = \theta(1+u)^p, \quad (\Gamma,\, \beta > 0).$$

When $p < 0$ the model (1) represents the tension-enhancing (cooperative) case and when $p > 0$ it describes the tension-inhibitive (activator-inhibitor) case. The current work is focused on the tension inhibitive case.

As opposed to tension-enhancing case, the tension-inhibitive case results in non-monotone traveling waves that are a better reflection of the real-life observations. Non-monotone traveling waves were explored numerically in [8]. Their analytic study is in the center of the presentation. More precisely, in [1] we prove the existence of traveling waves in two sub-regimes of the tension-inhibitive case. For both sub-regimes, we mainly use Geometric Singular Perturbation theory [4, 6] applied to the dynamical system that captures traveling wave solutions in (1) as its heteroclinic orbits.

One of the sub-regimes is when the spatial spreads of the level of unrest and the social tension are small. In this case, the parameter that sets the timescale over which the bandwagon effect would be observed, denoted by ω, plays a key role in the analysis. Specifically, we consider the singular limits as $\omega \to 0$ and $\omega \to \infty$ to find the appropriate heteroclinic orbits. We then use the theory of rotated vector fields [7] for the intermediate values of ω. In the limit as $\omega \to 0$ the dynamics of the system are driven mostly by the dynamics of u. On the other hand, as $\omega \to \infty$, the dynamics of the system are driven by the dynamics of v. This is aligned with the real-life expectations.

The second sub-regime is when the social tension diffuses at a much slower rate than the level of unrest. Using Geometric Singular Perturbation theory, the dynamics in this case can be reduced to an equation for the level of unrest which in under additional assumptions on β and p is a generalized Fisher-KPP equation. The heteroclinic orbit in the limiting Fisher-KPP equation is shown to persist in the perturbed system. Thus, we identify a regime when a traveling wave exists in the model (1).

Further directions of the research include investigating the stability of the traveling waves in either of the sub-regimes. Moreover, it would be interesting to relate the stability properties and the speed of propagation of the wave in second sub-regime to the stability and the speed of propagation of the wave in the limiting Fisher-KPP equation.

References

[1] M. Bakhshi, A. Ghazaryan, V. Manukian, N. Rodríguez. *Traveling wave solutions in a model for social outbursts in a tension-inhibitive regime*, Studies in Applied Mathematics. **147:2**(2021), 650–674.

[2] H. Berestycki, J.-P. Nadal, and N. Rodríguez. *A model of riot dynamics: shocks, diffusion, and thresholds*, Networks and Heterogeneous Media **3**(2015) 1–34.

[3] R. A. Fisher. *The wave of advance of advantageous genes*, Ann. Eugenics **7**(1937) 353–369.

[4] C. Jones. *Geometric singular perturbation theory*, in *Dynamical Systems (Montecatini Terme, 1994), Lecture Notes in Math. Springer, Berlin.* **1609**(1995) 44–118.

[5] A. Kolmogorov, I. Petrovskii, and N. Piskunov. *A study of the diffusion equation with increase in the amount of substance, and its application to a biological problem*, in V. M. Tikhomirov, editor, Selected Works of A. N. Kolmogorov I, 248–270. Kluwer 1991.

[6] C. Kuehn. *Multiple Time Scale Dynamics*, Springer, New York, 2015.

[7] L. M. Perko. *Rotated vector fields*, J. Differ. Equ. **103**(1993) 127–145.

[8] C. Yang and N. Rodríguez, *A Numerical Perspective on traveling wave solutions in a system for rioting activity*, Applied Mathematics and Computation, **364**(2020), 1–20.

Reporter: Paul Holst

Participants

Prof. Dr. Daniele Avitabile
Department of Mathematics
Vrije University
De Boelelaan 1081 a
1081 HV Amsterdam
NETHERLANDS

Dr. Bente Bakker
Mathematisch Instituut
Universiteit Leiden
Postbus 9512
2300 RA Leiden
NETHERLANDS

Prof. Dr. Margaret Beck
Department of Mathematics and
Statistics
Boston University
111 Cummington Mall
Boston, MA 02215-2411
UNITED STATES

Prof. Dr. Dirk Blömker
Institut für Mathematik
Universität Augsburg
86135 Augsburg
GERMANY

Prof. Dr. Jason Bramburger
University of Washington
Seattle, WA 98105
UNITED STATES

Dr. Maxime Breden
Centre de Mathématiques Appliquées
UMR CNRS 7641
École Polytechnique
Route de Saclay
91128 Palaiseau Cedex
FRANCE

Prof. Dr. Paul Carter
Department of Mathematics
University of Minnesota
127 Vincent Hall
206 Church Street S. E.
Minneapolis, MN 55455-0436
UNITED STATES

Dr. Martina Chirilus-Bruckner
Mathematisch Instituut
Universiteit Leiden
Postbus 9512
2300 RA Leiden
NETHERLANDS

Prof. Dr. Jonathan Dawes
Department of Mathematical Sciences
University of Bath
Claverton Down
Bath BA2 7AY
UNITED KINGDOM

Dr. Björn de Rijk
Fachbereich Mathematik
Universität Stuttgart
Pfaffenwaldring 57
70569 Stuttgart
GERMANY

Dr. Stephanie Dodson
Department of Mathematics
University of California, Davis
1, Shields Avenue
Davis, CA 95616-8633
UNITED STATES

Prof. Arjen Doelman
Mathematisch Instituut
Universiteit Leiden
Postbus 9512
2300 RA Leiden
NETHERLANDS

Prof. Dr. Bernold Fiedler
Institut für Mathematik I (WE 1)
Freie Universität Berlin
Arnimallee 2-6
14195 Berlin
GERMANY

Prof. Dr. Thierry Gallay
Institut Fourier
Université Grenoble Alpes
100, rue de Maths
38610 Gières Cedex
FRANCE

Dr. Anna Geyer
Delft Institute of Applied Mathematics
and Computer Science
Delft University of Technology
Van Mourik Broekmanweg 6
2628 XE Delft
NETHERLANDS

Dr. Anna R. Ghazaryan
Department of Mathematics
Miami University
Oxford OH 45056
UNITED STATES

Dr. Manuel Gnann
Delft Institute of Applied Mathematics
Faculty of Electrical Engineering,
Mathematics and Computer Sciences
Delft University of Technology
Van Mourik Broekmanweg 6
P.O. Box P.O. Box 5031
2600 GA Delft
NETHERLANDS

Dr. Ryan Goh
Department of Mathematics
Boston University
111 Cummington Street
Boston, MA 02215-2411
UNITED STATES

Prof. Dr. Mariana Haragus
Institut FEMTO-ST
Université de Franche-Comté
15b avenue des Montboucons
25030 Besançon Cedex
FRANCE

Paul Holst
Fachbereich 3 -
Mathematik und Informatik
Universität Bremen
Postfach 33 04 40
28334 Bremen
GERMANY

Dr. Matt Holzer
Department of Mathematical Sciences,
MS: 3F2
George Mason University
4400 University Drive
Fairfax VA 22030-4444
UNITED STATES

Dr. Hermen Jan Hupkes
Mathematisch Instituut
Universiteit Leiden
Postbus 9512
2300 RA Leiden
NETHERLANDS

Dr. Annalisa Iuorio
University of Vienna
Lederergasse 20/16
1080 Wien
AUSTRIA

Dr. Jonathan Jaquette
Department of Mathematics and
Statistics
Boston University
111 Cummington Mall
Boston, MA 02215-2411
UNITED STATES

Dr. Gabriela Jaramillo
Department of Mathematics
University of Houston
3551 Cullen Blvd.
Houston, TX 77204-3008
UNITED STATES

Prof. Dr. Christopher Jones
Renaissance Computing Institute
University of North Carolina
at Chapel Hill
100 Europa Dr Suite 540
Chapel Hill, NC 27517
UNITED STATES

Prof. Dr. Tasso J. Kaper
Department of Mathematics
Boston University
111 Cummington Street
Boston, MA 02215-2411
UNITED STATES

Prof. Dr. Panos Kevrekidis
Department of Mathematics
University of Massachusetts
Lederle Graduate Research Tower
710 North Pleasant Street
Amherst, MA 01003-9305
UNITED STATES

Dr. Sandra Kliem
Institut für Mathematik
Goethe-Universität Frankfurt
Robert-Mayer-Str. 10
60325 Frankfurt am Main
GERMANY

Prof. Dr. Edgar Knobloch
Department of Physics
University of California, Berkeley
376 Le Conte Hall
Berkeley CA 94720-3840
UNITED STATES

Prof. Dr. Theo Kolokolnikov
Department of Mathematics
Dalhousie University
Halifax NS B3H 3J5
CANADA

Prof. Dr. Christian Kühn
Zentrum Mathematik (M8)
TU München
Boltzmannstr. 3
85748 Garching bei München
GERMANY

Prof. Dr. Yuri Latushkin
Department of Mathematics
University of Missouri-Columbia
202 Mathematical Science Bldg.
Columbia, MO 65211-4100
UNITED STATES

Dr. Jean-Philippe Lessard
Dept. of Mathematics and Statistics
McGill University
805, Sherbrooke Street West
Montréal QC H3A 2K6
CANADA

Dr. David J. B. Lloyd
Dept. of Mathematics
University of Surrey
Guildford Surrey GU2 7XH
UNITED KINGDOM

Dr. Bing-Ying Lu
Fachbereich 3 -
Mathematik und Informatik
Universität Bremen
Postfach 33 04 40
28334 Bremen
GERMANY

Prof. Dr. Carl Mueller
Department of Mathematics
University of Rochester
Rochester, NY 14627
UNITED STATES

Dr. Claudio Munoz
Departamento Ingenieria Matematica
Universidad de Chile
Beauchef 851
Torre Norte, Piso 5
8370456 Estación Central Santiago
CHILE

Prof. Dr. Yasumasa Nishiura
Mid-Campus Open Laboratory Building No.2
Research Institute for Electronic Science
Hokkaido University
N12 W7, Kita-ku
Sapporo 060-0812
JAPAN

Dr. Antoine Pauthier
Fachbereich 3
Mathematik und Informatik
Universität Bremen
Postfach 330440
28334 Bremen
GERMANY

Prof. Dr. Jens Rademacher
Fachbereich 3 -
Mathematik und Informatik
Universität Bremen
Postfach 33 04 40
28334 Bremen
GERMANY

Prof. Dr. Wolfgang Reichel
Institut für Analysis
Karlsruher Institut für Technologie (KIT)
Englerstraße 2
76131 Karlsruhe
GERMANY

Prof. Dr. Vivi Rottschäfer
Mathematisch Instituut
Universiteit Leiden
Postbus 9512
2300 RA Leiden
NETHERLANDS

Prof. Dr. Björn Sandstede
Division of Applied Mathematics
Brown University
Box F
182 George St.
Providence, RI 02912
UNITED STATES

Prof. Dr. Arnd Scheel
School of Mathematics
University of Minnesota
127 Vincent Hall
206 Church Street S.E.
Minneapolis MN 55455-0436
UNITED STATES

Prof. Dr. Katharina Schratz
Laboratoire Jacques-Louis Lions
Sorbonne Université
4, place Jussieu
75252 Paris Cedex 05
FRANCE

Dr. Cinzia Soresina
Institut für Mathematik und wissenschaftliches Rechnen
Universität Graz
Heinrichstrasse 36
8010 Graz
AUSTRIA

Dr. Takashi Teramoto
School of Medicine
Asahikawa Medical University
2-1-1-1, Midorigaoka-higashi
Asahikawa 078-8510
JAPAN

Prof. Dr. Hannes Uecker
Institut fuer Mathematik
Carl v. Ossietzky-Universität Oldenburg
Fakultät V: Mathematik & Naturwissensch.
26111 Oldenburg
GERMANY

Prof. Dr. Jan Bouwe van den Berg
Department of Mathematics
Vrije Universiteit Amsterdam
de Boelelaan 1111
1081 HV Amsterdam
NETHERLANDS

Prof. Dr. Peter J.A. van Heijster
Mathematical and Statistical Methods
Biometris
Wageningen University and Research
P.O. Box 16
6708 PB Wageningen
NETHERLANDS

Dr. Frits W. J. Veerman
Mathematisch Instituut
Universiteit Leiden
Niels Bohrweg 1
2333 CA Leiden
NETHERLANDS

Prof. Dr. Clarence Eugene Wayne
Department of Mathematics and
Statistics
Boston University
111 Cummington Mall
Boston, MA 02215-2411
UNITED STATES

Dr. Martin Wechselberger
School of Mathematics & Statistics
The University of Sydney
Sydney NSW 2006
AUSTRALIA

Prof. Dr. J. Douglas Wright
Department of Mathematics
Drexel University
Korman Center 269
3141 Chestnut St.
Philadelphia, PA 19104
UNITED STATES